

From individual-based epidemic models to McKendrick-von Foerster PDEs: A guide to modeling and inferring COVID-19 dynamics

Félix Foutel-Rodier^{*,1,2} François Blanquart^{1,3} Philibert Courau¹
Peter Czuppon^{1,4} Jean-Jil Duchamps^{1,2} Jasmine Gamblin¹
Élise Kerdoncuff^{1,5} Rob Kulathinal^{1,6} Léo Régnier¹
Laura Vuduc¹ Amaury Lambert^{**,1,2} Emmanuel Schertzer^{**,1,2}

December 5, 2020

* first author

** co-last authors

¹ SMILE Group, Center for Interdisciplinary Research in Biology (CIRB), Collège de France, CNRS UMR 7241, INSERM U 1050, PSL Research University, Paris, France

² Laboratoire de Probabilités, Statistique & Modélisation (LPSM), Sorbonne Université, CNRS UMR 8001, Université de Paris, Paris, France

³ Infection, Antimicrobials, Modeling, Evolution (IAME), Université de Paris, INSERM UMR 1137, Paris, France

⁴ Institute of Ecology and Environmental Sciences of Paris (IEES), Sorbonne Université, UPEC, CNRS UMR 7618, IRD, INRA, Paris, France

⁵ Institut de Systématique, Biodiversité, Évolution (ISYEB), Muséum National d'Histoire Naturelle (MNHN), CNRS UMR 7205, Paris, France

⁶ Department of Biology, Temple University, Philadelphia, PA, USA

Abstract

We present a unifying, tractable approach for studying the spread of viruses causing complex diseases that require to be modeled using a large number of types (e.g., infective stage, clinical state, risk factor class). We show that recording each infected individual's infection age, i.e., the time elapsed since infection,

1. The age distribution $n(t, a)$ of the population at time t can be described by means of a first-order, one-dimensional partial differential equation (PDE) known as the McKendrick-von Foerster equation.
2. The frequency of type i at time t is simply obtained by integrating the probability $p(a, i)$ of being in state i at age a against the age distribution $n(t, a)$.

The advantage of this approach is three-fold. First, regardless of the number of types, macroscopic observables (e.g., incidence or prevalence of each type) only rely on a one-dimensional PDE “decorated” with types. This representation induces a simple methodology based on the McKendrick-von Foerster PDE with Poisson sampling to infer and forecast the epidemic. We illustrate this technique using a French data from the COVID-19 epidemic.

Second, our approach generalizes and simplifies standard compartmental models using high-dimensional systems of ordinary differential equations (ODEs) to account for disease complexity. We show that such models can always be rewritten in our framework, thus, providing a low-dimensional yet equivalent representation of these complex models.

Third, beyond the simplicity of the approach, we show that our population model naturally appears as a universal scaling limit of a large class of fully stochastic individual-based epidemic models, where the initial condition of the PDE emerges as the limiting age structure of an exponentially growing population starting from a single individual.

Ch

1	Introduction	3
1.1	Challenges posed by complex diseases such as COVID-19	3
1.2	Generic model assumptions	4
1.3	Statement of results and outline	5
1.4	Natural extensions	7
1.5	Compartmental ODE models	8
1.6	Relation with previous works	10
2	Two Feynman-Kac formulae	11
2.1	Assumptions and notation	11
2.2	McKendrick-von Foerster PDE: Weak solutions	13
2.3	A forward Feynman-Kac formula	14
2.4	Dual CMJ process and backward Feynman-Kac formula	18
3	Two laws of large numbers	20

4 Inference	25
4.1 Case study: the French COVID-19 epidemic	25
4.2 The model	25
4.3 Parametrization of the model	26
4.4 Fitting the model to incidence data	27
A Maximum likelihood method	37
B Best fitting prevalence curves under admission model	37

1 ~~Id~~

1.1 Challenges posed by complex diseases such as COVID-19

The transmission of pathogens between species is a global concern [1, 2]. As such zoonotic episodes are expected to become increasingly common in humans, it is critical to develop analytic tools that can quickly transform epidemiological observations into informed public policy in order to mitigate and control epidemics.

A novel coronavirus, SARS-CoV-2, has recently crossed the species barrier into humans and, within months, has rapidly spread to all corners of our planet [3]. The sheer scale of this pandemic has overburdened our medical infrastructure, caused fatalities estimated well into the hundreds of thousands, and shut down entire economies. Remarkably, the rapid spread of COVID-19 and its consequences can be attributed to the unique life cycle of a 30,000 base pair single-stranded virus. SARS-CoV-2 is an airborne pathogen transmitted by both symptomatic and asymptomatic carriers in close proximity to non-infected individuals. Milder COVID-19 symptoms include a dry cough, fever, and/or shortness of breath while more serious cases include respiratory failure and eventual death. With millions of infections and hundreds of thousands of documented deaths and recoveries, the COVID-19 pandemic is providing a wealth of independent estimates of important clinical characteristics that can help predict health outcomes specific for a country or region.

It quickly became understood that accurate descriptions of the life cycle of this disease needed to distinguish between several stages of the disease, referred to as compartments, depending on whether an infected individual is infectious or not, symptomatic or not, hospitalized, *etc.* However it remains unclear to what extent making precise predictions of the dynamics of such a complex disease requires to have a precise knowledge of clinical features such as incubation period, generation time, and duration times between infection, symptom establishment, hospitalization, recovery and death, to know how these durations correlate and what are the exact probabilities of transition between stages.

In this work, we consider a fully stochastic, generic epidemiological model with an arbitrary number of compartments, that encompasses life cycles of most complex diseases and that of COVID-19 in particular. We show how structuring the infected population by its infection age, i.e., time elapsed since infection, allows us to decouple dependencies between stages and to time. More specifically, when the population size is large enough, the joint evolution of all compartment sizes can be described by means of a linear, first-order partial differential equation (PDE) known as the McKendrick-von Foerster equation describing the number $n(t, a)$ of infecteds of (infection) age a at time t . The boundary condition at age 0 is driven by the infection rate from infecteds of age a *averaged* over all

life cycles and the number of individuals of age a in compartment i at time t is obtained by thinning $n(t, a)$ by a factor $p(a, i)$ which is the probability of being in compartment i conditional on having age a , *averaged* over all life cycles.

In the case of COVID-19, we display a simple procedure to infer these parameters, some from the biological literature and most from time series of numbers of severe cases, hospitalized cases, discharged patients and deaths that can be applied easily to any regional or national dataset. We also allow for time inhomogeneity in the infection rate to account for temporary mitigation measures such as lockdowns or social distancing. We apply this procedure to French COVID-19 data from March to May 2020 and estimate various parameters of interest including R_0 in different phases of the epidemic (before, during, and after lockdown) and biological parameter values that we compare to empirical estimates.

1.2 Generic model assumptions

We consider a population model of the SIR fashion where each individual goes through successive stages, starting from stage S (susceptible) and ending in one of two states: R (recovered) or D (dead). Depending on disease complexity, the number of stages in this life cycle can vary. In the SARS-CoV-2 example, typical intermediate stages are A (asymptomatic) or P (presymptomatic), I (mild case) or C (severe case), H (hospitalized), U (intensive care unit). These stages are sometimes called compartments, types, classes, stages or simply states. See Figure 4 for an illustration.

We assume that S individuals are always in excess (branching assumption) and that each individual infects new S individuals at successive times of a random point process, one at a time. We further assume that upon infection, an S individual immediately changes state and never returns to state S (ruling out multiple infections in particular). More formally,

- The set of all possible states is denoted \mathcal{S} and a stochastic process $(X(a); a \geq 0)$ with values in \mathcal{S} gives the state of a typical individual of age a , where here *age* means *age of infection*, i.e., time elapsed since infection. For the sake of simplicity, we will assume that \mathcal{S} is a discrete space.
- A random point measure \mathcal{P} describes the times of secondary infections. Due to the previous assumptions, atoms of \mathcal{P} all have mass 1 and only charge $(0, \infty)$.
- We can (and will) superimpose time heterogeneity to this process by means of a *suppression function* $(c(t); t \geq 0)$ valued in $[0, 1]$ thinning the infection process. More precisely, if t is a potential time of infection for individual x (i.e., t is an atom of its infection point process \mathcal{P}_x), we ignore the event with probability $1 - c(t)$. This suppression function can model the effect of vaccination, of density-dependence (i.e., relaxing the branching assumption due to an excess of removed or of deceased individuals), or of governmental mitigation measures (i.e., social distancing, lockdown).

The population is thus described by a *Crump-Mode-Jagers branching process*, where all individuals x are characterized by independent copies (\mathcal{P}_x, X_x) of the pair (\mathcal{P}, X) describing, respectively, the process of infection and the life cycle. In the branching process literature, X is often referred to as a *random characteristic* of individual x [4, 5, 6].

Remark 1. *A typical infection measure is a Poisson Point Process with intensity λ killed at an independent exponential random variable with parameter γ . (By killing we mean that we erase all atoms of the PPP after the killing time.) This corresponds to the classical SIR process with rate of infection λ and recovery rate γ . More generally, we can construct a SEIR process (E for exposed) as follows. Let L be a random variable and consider ξ be a Poisson Point Process with an intensity measure $\lambda(x)dx$. Then define $\mathcal{P}([a, b]) = \xi([(a - L)^+, (b - L)^+])$ so that no infection occurs during the incubation period $[0, L]$.*

Remark 2. *\mathcal{P} and X are generally not independent. As a simple example, since (most) diseases cannot be transmitted by deceased individuals, no atom of \mathcal{P} is allowed once X has reached the end-state D . In the same spirit, one could assume that the infection potential of a given individual is reduced once in the hospital and that individuals with many atoms in their infection process \mathcal{P} (high infectiosity) are identified and isolated.*

Remark 3. *Classes such as P , I or H must sometimes be refined to account for additional structuring variables like general health condition, (real) age, spatial position or previous exposure to similar pathogen. Knowledge of such variables can help predict more accurately the outcome of the infection and parametrize more precisely the infection process. Regarding this last point, note that the assumptions in force here allow for any implicit or explicit structure provided that transmission from an individual of type i to an individual of type j does not depend on j (but may depend on i , as we have seen). Relaxing this assumption would result in describing the large population limit by a multidimensional PDE instead of a one-dimensional PDE (see Section 1.4). Also, note that ignoring structuring by a hidden variable such as spatial position or health condition can lead to difficulties in estimating sojourn times in each compartment (such as P , I or H) from clinical data, due to over- or under-representation in this compartment of subsets of individuals carrying certain values of the hidden variable.*

1.3 Statement of results and outline

The stochastic epidemic models we consider here are fairly general and can exhibit quite complex dependencies (i) between states and time, due to the lack of any Markov-type assumption, (ii) between states, due to possibly hidden structuring variables impacting the life cycle, (iii) between state and infection rate, and (iv) between past and future infection events. The main message of this note is that despite this apparent complexity, most of this complexity vanishes when the size of the population is large. More specifically, we show that in the limit of large populations (obtained by starting from a large initial population or as a consequence of natural exponential growth), the population of infecteds structured by age (of the infection) can be described by a one-dimensional PDE that only depends on

- (a) The average infection rate

$$\tau(da) := \mathbb{E}(\mathcal{P}(da)),$$

and

- (b) The 1d marginals of the life-cycle process

$$p(a, i) := \mathbb{P}(X(a) = i).$$

Large initial population. Let us start with N infected individuals and define the empirical measure μ_t^N describing the ages and types of infected individuals present at time t

$$\mu_t^N(\mathrm{d}a \times \{i\}) := \sum_x 1_{\sigma_x < t} \delta_{(t-\sigma_x, X_x(t-\sigma_x))}(\mathrm{d}a \times \{i\}), \quad (1)$$

where the sum is taken over all individuals x having ever lived and σ_x denotes the birth (infection) time of x . According to our first result (Theorem 7), starting from N infected individuals at time 0 with i.i.d. infection ages with law g , we have the a.s. convergence

$$\lim_{N \rightarrow \infty} \frac{1}{N} \mu_t^N(\mathrm{d}a \times \{i\}) = n(t, a) p(a, i) \mathrm{d}a,$$

where $n(t, a)$ solves the McKendrick-von Foerster PDE

$$\begin{aligned} \forall t, a > 0, \quad \partial_t n(t, a) + \partial_a n(t, a) &= 0 \\ \forall t > 0, \quad n(t, 0) &= c(t) \int_0^\infty \tau(\mathrm{d}a) n(t, a), \\ \forall a \geq 0, \quad n(0, a) &= g(a). \end{aligned} \quad (2)$$

After lockdown. Our second result (Theorem 8) displays a similar, but more subtle, convergence in the case when the process is supercritical, where natural growth leads by itself to large population sizes. Let $Z(t)$ denote the total population size at time t and assume that $Z(0) = 1$, i.e., we start from a *single individual*. By a slight abuse of notation, denote by $\mu_t^{t_K}$ the empirical measure of ages and types as in (1), but under the assumption that the suppression function at time t is equal to $c(t - t_K)$ where c is equal to 1 for negative arguments, and t_K is some large, random time. We are motivated by modeling a situation where the infection is separated into two distinct phases:

- (Phase 1) We let the epidemic develop until a certain random time t_K . For instance, t_K could be the time at which the number of recorded deaths exceeds a large threshold K . We assume no suppression before t_K ;
- (Phase 2) We let the suppression function vary after time t_K , e.g., due to mitigation measures and/or behavioral changes (i.e., lockdown phase).

Conditional on non-extinction, letting (t_K) be any sequence of stopping times such that $t_K \rightarrow \infty$ on the non-extinction event, we have the following convergence in probability

$$\lim_{K \rightarrow \infty} \frac{\mu_{t_K+t}^{t_K}}{Z(t_K)} = n(t, a) p(a, i) \mathrm{d}a.$$

Now $n(t, a)$ solves the McKendrick-von Foerster PDE with the same boundary condition as previously, but with initial condition $n(0, a) = \alpha e^{-\alpha a}$, where $\alpha > 0$ is the exponential growth rate of $Z(t)$ for $t \leq t_K$, also called Malthusian parameter. This second result can be seen as a refinement of limit theorems for exponentially growing populations counted with random characteristics, where here the characteristic of a typical individual is the number of her descendants in class i of age a , born at least s time units after her birth (summed over $s_x = t_K - \sigma_x$). In particular, taking $t = 0$ in the statement yields the

convergence to the exponential stable age distribution decorated by the 1d marginals p of X . The way we state the result nicely displays dependencies between characteristics corresponding to different t 's.

To summarize: (1) *the macroscopic infection process is characterized by the sole intensity measure τ and dictates an explicit age structure of the population, and (2) the class structure is deduced by averaging the life-cycle process against the limiting age profile.* In order to validate our approach, we use those deterministic approximations to infer epidemiological parameters (R_0 before and during lockdown) from recent empirical observations, and show that our findings are in accordance with the current literature.

Outline. The paper is organized as follows. In Section 2, we study the McKendrick-von Foerster equation (2). After providing a precise description of the branching process that we are considering in Section 2.1, we give the definition of a weak solution to (2) in Section 2.2. Then, we give two probabilistic representations of these weak solutions. We first show in Section 2.3 that the weak solution to (2) corresponds to the first moment of the branching process that we are studying, when viewed as a random measure on the ages of infection. Second, Section 2.4 provides a construction of the weak solution using a dual genealogical process. The two laws of large numbers are proved in Section 3. Finally the inference is carried out in Section 4. Section 4.2 and Section 4.3 describe our choice of parametrization and the inference results are discussed in Section 4.4.

1.4 Natural extensions

Some of the assumptions underlying the previous models can be relaxed and our general framework can be adapted to more complex and realistic populations.

Contact matrix. So far, infectious individuals infect new individuals uniformly at random. In general, a contact matrix specifies the contact rate, depending on contact location (household, school, work...) or individual types of source and target (real age, susceptibility...) [7, 8]. More precisely, each individual now belongs to one class, and we denote by \mathcal{C} the (finite) set of all classes. An individual in class $j \in \mathcal{C}$ is characterized by a multi-dimensional process $(X^j, \mathcal{P}^{j,1}, \dots, \mathcal{P}^{j,C})$ where the atoms of $\mathcal{P}^{j,k}$ provide the age at which this individual infects a new individual of type $k \in \mathcal{C}$, and $(X^j(a); a \geq 0)$ is a \mathcal{S} -valued process whose distribution can depend on j .

We define the mean contact matrix as

$$\forall j, k \in \mathcal{C}, \quad \tau^{jk}(du) := \mathbb{E}(\mathcal{P}^{j,k}(du)).$$

The population is again described by a multi-type Crump-Mode-Jagers branching process. Analogously to (1), $\mu_t^{\mathbf{N},j}$ denotes the empirical measure of j individuals starting with $\mathbf{N} = (N^j)_{j \in \mathcal{C}}$ infected individuals at time $t = 0$. Assume that there exists a constant N such that for all $j \in \mathcal{C}$, $N^j/N \rightarrow y^j$ as $N \rightarrow \infty$. Under the usual technical conditions (the matrix τ is irreducible and Malthusian, $x \log(x)$ type condition, see [9]),

$$\forall j \in \mathcal{C}, \forall i \in \mathcal{S}, \quad \frac{1}{N^j} \mu_t^{\mathbf{N},j}(da \times \{i\}) \implies n^j(t, a) \mathbb{P}(X^j(a) = i) da$$

where $(n^j)_{j \in \mathcal{C}}$ satisfies the multidimensional McKendrick-von Foerster equation

$$\begin{aligned} \partial_t n^j(t, a) + \partial_a n^j(t, a) &= 0 \\ \forall t > 0, \quad n^j(t, 0) &= \sum_{k \in \mathcal{C}} c^{kj}(t) \int_0^\infty \tau^{kj}(da) n^k(t, a), \\ \forall a \geq 0, \quad n^j(0, a) &= y^j g^j(a). \end{aligned} \tag{3}$$

where g^j describes the initial age profile of class j and $c^{jk}(t)$ is a matrix at time t generalizing the suppression function of the previous section. Following Theorem 8, it is natural to consider the initial condition

$$g^j(u) = \alpha \exp(-\alpha u) \phi^j$$

where α is the Malthusian parameter, i.e. the unique α such that the largest eigenvalue of the matrix

$$\int \exp(-\alpha u) \tau(du)$$

is equal to 1 and $(\phi^j)_{j \in \mathcal{C}}$ is its Perron-Frobenius left eigenvector with (positive) entries summing up to 1. As in Theorem 8, such initial condition can be justified by starting with a single individual and let the population grow up to a large random time t_K conditional on non-extinction [9].

Shortage of susceptibles. Another natural extension consists in taking into account saturation of infected in the population. Start with a finite, but large population of size N with a fraction of infected individuals $x \in (0, 1)$ with an age profile g at time $t = 0$. Here infection is only effective if the target individual is susceptible, which thins infection rate by the fraction of susceptibles in the population. At the limit, this saturation translates into a non-linear McKendrick-von Foerster equation

$$\begin{aligned} \forall t, a > 0, \quad \partial_t n(t, a) + \partial_a n(t, a) &= 0 \\ \forall t > 0, \quad n(t, 0) &= S(t) c(t) \int_0^\infty \tau(da) n(t, a), \\ \forall a \geq 0, \quad n(0, a) &= x g(a), \end{aligned} \tag{4}$$

where we have defined

$$S(t) := 1 - \int_0^\infty n(t, a) da,$$

and the limiting empirical measure is given by $n(t, a) p(a, j) da$. Convergence results to this limiting PDE are addressed by some of the present authors in [10].

1.5 Compartmental ODE models

An important special case of our model is when the process $(X(a); a \geq 0)$ is a Markov process and infections from individual x occur at a rate that only depends on the current state of x .

Under these assumptions, the McKendrick-von Foerster PDE reduces to a finite set of ODEs. Similar sets of ODEs have been widely used to model the SARS-CoV-2 epidemic [11, 12, 13, 14], and in that sense, *taking into account explicitly the (infection) age*

structure of the population allows us to incorporate all these models into the same general framework.

More precisely, for $i \in \mathcal{S}$ define

$$\forall t \geq 0, \quad N_i(t) = \int_0^\infty n(t, a)p(a, i)da$$

to be the number of individuals in state i . We will assume that $(X(a); a \geq 0)$ is a Markov process with transitions $(\lambda_{ij})_{i, j \in \mathcal{S}}$. Moreover, we suppose that conditional on $(X(a); a \geq 0)$, the infection process \mathcal{P}_x from individual x is a Poisson point process with intensity rate τ_i when x is in state i . Then a direct computation shows the following result.

Proposition 1. *Suppose that $(X(a); a \geq 0)$ is a Markov process with transitions $(\lambda_{ij})_{i, j \in \mathcal{S}}$, and that conditional on $(X(a); a \geq 0)$, \mathcal{P} is a Poisson point process with intensity $(\tau_{X(a)}; a \geq 0)$. Then, if $(n(t, a))$ denotes the solution to (4), $(N_i(t); t \geq 0)_{i \in \mathcal{S}}$ solves the following set of ODE:*

$$\forall i \in \mathcal{S}, \quad \dot{N}_i = \sum_{j \in \mathcal{S}} \lambda_{ji} N_j - N_i \sum_{j \in \mathcal{S}} \lambda_{ij} + \sum_{j \in \mathcal{S}} a_{ji} N_j S, \quad (5)$$

where $a_{ji} := \tau_j p(0, i)$ and $S := 1 - \sum_{i \in \mathcal{S}} N_i$.

Proof. Recall that

$$N_i(t) = \int_0^\infty n(t, a)p(a, i)da.$$

By differentiating both sides with respect to time we get

$$\begin{aligned} \dot{N}_i(t) &= \int_0^\infty \partial_t n(t, a)p(a, i)da = - \int_0^\infty \partial_a n(t, a)p(a, i)da \\ &= \int_0^\infty n(t, a)\partial_a p(a, i)da + n(t, 0)p(0, i). \end{aligned}$$

By using the boundary condition and the fact that $(X(a))_{a \geq 0}$ is a Markov process, we obtain that

$$\begin{aligned} \dot{N}_i(t) &= \int_0^\infty n(t, a) \left(\sum_{j \in \mathcal{S}} \lambda_{ji} p(a, j) - \lambda_{ij} p(a, i) \right) da + S(t)p(0, i) \int_0^\infty n(t, a) \sum_{j \in \mathcal{S}} \tau_j p(a, j) da. \\ &= \sum_{j \in \mathcal{S}} \lambda_{ji} N_j(t) - N_j(t) \sum_{j \in \mathcal{S}} \lambda_{ij} + \sum_{j \in \mathcal{S}} a_{ji} S(t) N_j(t), \end{aligned}$$

which ends the proof. \square

Conversely, let us consider from the start the system of ODEs (5). Here, λ_{ij} is interpreted as the rate at which a type i individual turns into type j and a_{ij} as the rate at which a type i individual gives birth to a type j individual. If the contact matrix with generic entries a_{ij} has rank 1 and non-negative entries, it can always be decomposed as $a_{ij} = \tau_i p(0, j)$ where $\tau_i \geq 0$ and $(p(0, j))$ is a probability vector. The vectors (τ_i) and $(p(0, j))$ can be recovered by

$$\tau_i = \sum_{j \in \mathcal{S}} a_{ij} \quad \text{and} \quad p(0, j) = \frac{a_{ij}}{\tau_i} \quad (\forall i, j).$$

Note that here $a_{ij} = \lambda(i)p(0, j)$, so that actually a type i individual gives birth at rate $\lambda(i)$ and her offspring has type independently distributed according to $p(0, \cdot)$. As a result, the contact matrix with generic entries a_{ij} has rank 1, and λ and $p(0, \cdot)$ can be recovered by

$$\lambda(i) = \sum_{j \in \mathcal{S}} a_{ij} \quad \text{and} \quad p(0, j) = \frac{a_{ij}}{\lambda(i)} \quad (\forall i, j).$$

Then one can define $(X(a); a \geq 0)$ as the \mathcal{S} -valued process with rates given by the matrix Λ (with diagonal entries $\lambda_{ii} = -\sum_{j \notin \mathcal{S}} \lambda_{ij}$) and initial distribution $(p(0, i))$. Denote as in the rest of the text

$$p(a, i) = \mathbb{P}(X(a) = i),$$

so that the row matrix $p(a, \cdot)$ can be computed as the product $p(0, \cdot) \exp(a\Lambda)$.

Now let us consider the solution $(N_i(t); t \geq 0)$ to (5) and assume there is some age distribution g (integrable but possibly not summing to 1) such that

$$N_i(0) = \int_0^\infty g(a)p(a, i)da. \quad (6)$$

Then by uniqueness of (N_i) and thanks to Proposition 1, for all $i \in \mathcal{S}$,

$$N_i(t) = \int_0^\infty n(t, a)p(a, i)da,$$

where n is the solution to the McKendrick-von Foerster PDE with initial condition g and boundary condition

$$n(t, 0) = \int_0^\infty \tau(a)n(t, a)da,$$

where $\tau(a) := \sum_{j \in \mathcal{S}} \tau_j p(a, j)$. This shows that the solution to any linear system of ODEs of the form (5) has a simple representation in terms of the solution to the McKendrick-von Foerster PDE decorated with types, provided there is a representation of the initial condition in the form (6). Note that this last property is not necessarily fulfilled. For example, if X is ergodic and started in its stationary probability distribution, then $p(a, i) = p(0, i)$ and (6) would only hold if $(n_i(0))_{i \in \mathcal{S}}$ were proportional to $(p(0, i))_{i \in \mathcal{S}}$.

If the matrix with generic entries a_{ij} does not have rank 1, one could derive a similar representation of the solutions to (5), but using the multi-dimensional version of the McKendrick-von Foerster equation (3).

1.6 Relation with previous works

Non-Markov epidemic models have already been investigated, see e.g. [15, 16, 17, 18]. The idea of representing a general branching population by its age structure has a rich history in probability theory [19, 20, 21, 22, 23, 24, 25, 26] and the connection with the McKendrick-von Foerster PDE has been acknowledged several times [20, 24]. In the latter two works, the authors allow for birth and death rates that may depend not only on abundances of each type, but also on the whole age structure of the population. This impressive level of generalization comes at the cost of assuming that the process describing the evolution of the empirical measure on ages and types is Markovian. In particular, birth and death rates are not allowed to depend on past individual birth events. The Markov property then allows the use of a generator for the empirical measure and with some

extra finite second moment assumptions on the intensity measure, this approach allows the authors to obtain a law of large numbers and a central limit theorem.

We acknowledge that the current work is certainly not as mathematically challenging as the works alluded to above, and that some of our results are almost implicit in some of the previous works. However, we believe that our point of view (1d PDE decorated with types) does deserve to be highlighted in the current sanitary crisis since it provides a natural and efficient inference methodology. More than 70,000 publications related to the COVID-19 crisis have appeared since the onset of the pandemic, with many different modeling approaches. One of the modest aims of the present note is to convey the idea that individual-based stochastic models suggest a simple and tractable framework for tackling some of the complex features of the disease. Furthermore, since we ignore finite population effects, our proofs are quite elementary compared to [20, 24] and should be accessible to a much wider audience interested in such a modeling approach.

Finally, we already pointed out that the connection between branching processes and McKendrick-von Foerster PDE has been discussed in previous works. However, as far as we can tell, the duality result exposed in Section 2.4 is new and can presumably be extended to more general branching processes where birth and death rates are allowed to be frequency-dependent. In [10], some of the authors of the present work show that this duality result has a natural counterpart in a model with a finite but large population.

2 ~~of Ken~~

2.1 Assumptions and notation

CMJ branching process with suppression. Recall that the infection process is modeled by a Crump-Mode-Jagers (CMJ) branching process [19, 4] with no death, starting from one individual called the progenitor (or root of the tree). Each individual x is characterized by an independent pair (\mathcal{P}_x, X_x) embodying respectively the processes of secondary infection events from x and of types carried by x . Each pair (\mathcal{P}_x, X_x) is a copy of the pair (\mathcal{P}, X) with law \mathcal{L} , except when x is the root, where it is distributed as $(\tilde{\mathcal{P}}, \tilde{X})$ with law $\tilde{\mathcal{L}}$ (more on that below).

Also recall some infection events can be suppressed using a suppression function $(c(t); t \geq 0)$. Given a realization of the CMJ tree, for each branching point occurring at time t , we trim the tree by independently pruning the subtree stemming from it with probability $c(t)$. See Figure 1.

For simplicity, we will assume that the suppression function c is a piecewise right-continuous function, and that for any $t \geq 0$, the process $(X(a); a \geq 0)$ is a.s. continuous at t . Define the average infection measure (that is, the intensity measure of the point process \mathcal{P}) as

$$\tau(du) := \mathbb{E}(\mathcal{P})(du).$$

We assume that τ is absolutely continuous w.r.t. the Lebesgue measure in such a way that there exists a measurable non-negative function β such that

$$\tau(du) = \beta(u)du \quad \text{and} \quad R_0 := \int_0^\infty \beta(u)du < \infty. \quad (7)$$

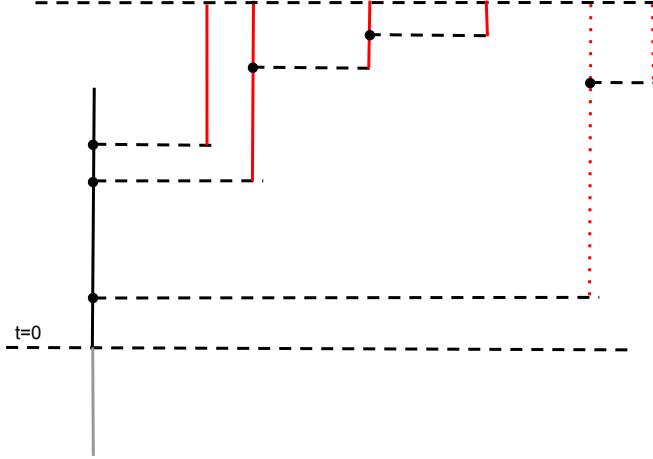


Figure 1: The initial individual $(\tilde{\mathcal{P}}, \tilde{X})$ is represented by a black segment. In Section 2.1, we assume that at time $t = 0$, the age of the initial individual (length of the grey segment) is distributed according to a probability density g . If a branching event is observed at time t (see e.g., black dots), the infection occurs with probability $c(t)$. In the CMJ, this amounts to prune the corresponding subtree with probability $c(t)$ (dotted red tree).

We also assume that there exists a unique parameter $\alpha \in \mathbb{R}$ (the so-called Malthusian parameter of the CMJ process) such that

$$\int \exp(-\alpha u) \tau(du) = 1. \quad (8)$$

The parameter α can be either positive (supercritical) or negative (subcritical). Finally, we will also enforce the Kesten and Stigum criterium [27]

$$\mathbb{E}(R_\alpha \log^+(R_\alpha)) < \infty, \quad (9)$$

where

$$R_\alpha := \int_0^\infty \exp(-\alpha t) \mathcal{P}(dt).$$

Initial shifted law. For any finite measure m on \mathbb{R}_+ , we define $\theta_t \circ m$ as the measure shifted by t , i.e.,

$$\int_0^\infty f(u) \theta_t \circ m(du) = \int_t^\infty f(u-t) m(du),$$

where f is any measurable, bounded function f on \mathbb{R}_+ . For any measurable function $F : \mathbb{R}_+ \rightarrow \mathcal{S}$, we similarly define $\theta_t \circ F$ by $\theta_t \circ F(u) = F(u+t)$. (We make a slight abuse of notation by using the same symbol for the shift operator on measures and functions.)

Let g be a probability density on \mathbb{R}_+ . We now specify the law $\tilde{\mathcal{L}}_g$ of the pair $(\tilde{\mathcal{P}}, \tilde{X})$ characterizing the root. In order to connect the CMJ process with the McKendrick-von Foerster equation, we will focus on the case where $(\tilde{\mathcal{P}}, \tilde{X})$ is identical in law to $(\theta_A \circ \mathcal{P}, \theta_A \circ X)$, where A is a r.v. independent of (\mathcal{P}, X) and distributed according to g . The distribution $\tilde{\mathcal{L}}_g$ will be referred to as the *shifted law*. In particular, we have

$$\tilde{\tau}(da) := \mathbb{E}(\tilde{\mathcal{P}}(da)) = \left(\int_0^\infty \beta(x+a) g(x) dx \right) da.$$

Notation. We assume that individuals are indexed by the standard Ulam-Harris labeling. Namely, individuals are indexed in $I = \cup_n (\mathbb{N}^*)^n$. If $x \in I$, then xi (the concatenation of x and i) is interpreted as the i -th child of x . Children are ranked according to their birth time: $(x, 1)$ is the oldest child of x , $(x, 2)$ the second oldest, *etc.* (Since we assumed that τ has a density, there is no simultaneous births and the atoms of \mathcal{P} are distinct a.s.) We denote by σ_x the date of birth of x with the convention that $\sigma_x = \infty$ if the individual is never born. For instance, if $\sigma_x < \infty$ and x has k children, then $\sigma_{x_j} = \infty$ for $j > k$. Finally, \emptyset will denote the root of the tree.

2.2 McKendrick-von Foerster PDE: Weak solutions

In this section, we consider the time-inhomogeneous, linear McKendrick-von Foerster PDE (2). The first line in (2) is the transport equation with unit velocity, i.e., ages of individuals increase at rate 1. The second line gives the number of newly infected individual (age 0) at time t .

In order to motivate our definition of weak solutions, we start by giving a formal resolution of the PDE using the method of characteristics. Fix $a > 0$. Let

$$A(t) = a - t$$

Then

$$\frac{d}{ds} n(t-s, A(s)) = -\partial_t n(t-s, A(s)) - \partial_a n(t-s, A(s)) = 0,$$

so that $s \mapsto n(t-s, a-s)$ is conserved along the characteristics, i.e.,

$$\forall s < a, \quad n(t, a) = n(t-s, a-s).$$

It follows that

$$n(t, a) = \begin{cases} g(a-t) & \text{when } a > t \\ b(t-a) & \text{when } a \leq t \end{cases} \quad (10)$$

where $b(t) = c(t) \int_0^\infty \tau(da) n(t, a)$. We now determine the function b . Injecting the previous expression into the ‘spatial’ boundary condition of the PDE, we obtain a delayed equation for b : for every $t > 0$

$$b(t) = c(t) \int_0^t \tau(da) b(t-a) + c(t) \int_t^\infty \tau(da) g(a-t). \quad (11)$$

Lemma 2. *There exists a unique solution b to (11) which is locally integrable. Moreover, for any $\delta \geq 0$ such that $\delta > \alpha$ we have $b \in \mathcal{L}^{1,\delta}$, where $\mathcal{L}^{1,\delta}$ denotes the set of all functions $f : \mathbb{R}_+ \rightarrow \mathbb{R}$ such that $\|f\|_{\mathcal{L}^{1,\delta}} := \int_0^\infty e^{-\delta t} |f(t)| dt < \infty$.*

Proof. Fix $\delta > \alpha$ and denote by $L^{1,\delta}$ the space $\mathcal{L}^{1,\delta}$ quotiented by the relation \sim_δ , where $f \sim_\delta g$ if $\|f - g\|_{L^{1,\delta}} = 0$. Then define the linear operator $\Phi : L^{1,\delta} \rightarrow L^{1,\delta}$ by

$$\Phi f : t \mapsto c(t) \int_0^t f(t-u) \beta(u) du.$$

Then we have

$$\begin{aligned}\|\Phi f\|_{L^{1,\delta}} &= \int_0^\infty e^{-\delta t} \Phi f(t) dt = \int_0^\infty e^{-\delta t} c(t) \int_0^t f(t-u) \beta(u) du dt \\ &= \int_0^\infty e^{-\delta u} f(u) \int_u^\infty \beta(t-u) e^{-\delta(t-u)} c(t) dt du.\end{aligned}$$

Now using that

$$\int_u^\infty \beta(t-u) e^{-\delta(t-u)} c(t) dt \leq \int_0^\infty \beta(t) e^{-\delta t} dt < 1$$

we obtain that $\|\Phi\| < 1$. Define

$$\Psi := \text{Id} - \Phi.$$

Then Ψ is invertible with inverse $\sum_{k \geq 0} \Phi^k$. Note that equation (11) can be written as

$$\Psi(b) = F,$$

where

$$F: t \mapsto c(t) \int_t^\infty \beta(a) g(t-a) da.$$

The proof ends noting that $F \in L^{1,\delta}$ as

$$\int_0^\infty e^{-\delta t} F(t) dt \leq \int_0^\infty \int_t^\infty \beta(a) g(t-a) da dt < \infty.$$

We have thus proved existence and uniqueness of the solution b to (11) in $L^{1,\delta}$. Now for any two functions b_1 and b_2 such that $b_1 \sim_\delta b_2$ and b_1 and b_2 both satisfy (11), we have $b_1 = b_2$ (i.e., there is a single element in the equivalence class of b). This shows uniqueness of the solution b to (11) in $\mathcal{L}^{1,\delta}$.

Since all elements of $L^{1,\delta}$ are locally integrable, this also shows the existence of a locally integrable solution to (11). Its uniqueness can be proved following the exact same reasoning as previously, replacing integrations on $[0, \infty)$ by integration on compact intervals. \square

Definition 3. We say that $(n(t, a); a, t \geq 0)$ is the $\mathcal{L}^{1,\text{loc}}$ weak solution to the McKendrick-von Foerster PDE with initial condition g if it satisfies the relation (10) where $(b(t); t \geq 0)$ is the unique locally integrable solution to (11) displayed in the previous lemma.

2.3 A forward Feynman-Kac formula

Define

$$Z(t) := \sum_x \mathbb{1}(\sigma_x \in (0, t]), \quad B(t) := \mathbb{E}(Z(t))$$

where $Z(t)$ is interpreted as the number of infections between 0 and t . Recall that $R_0 := \int_0^\infty \beta(u) du < \infty$ guarantees that $B(t) < \infty$ for all $t \geq 0$. Finally, B is non-decreasing and we denote by dB the Stieljes measure associated to B .

Lemma 4. There exists a locally integrable function $(b(t); t \geq 0)$ such that

$$dB(t) = b(t) dt.$$

Further, b coincides with the unique locally integrable solution of the delayed equation (11).

Proof. The fact that dB has a density easily follows from the fact that τ has a density. The fact that $B(t) < \infty$ ensures that b is locally integrable.

Define $\bar{\mathcal{P}}_x$ the infection measure obtained from \mathcal{P}_x after random thinning by the function $(c(t); t \geq 0)$. Namely, conditional on σ_x and the atoms $a_1 < a_2 < \dots$ of \mathcal{P}_x , we remove independently each of the atoms with respective probabilities $1 - c(\sigma_x + a_1), 1 - c(\sigma_x + a_2) \dots$, whereas the other atoms remain unchanged.

Fix $t > 0$. Let $k \leq n \in \mathbb{N}$. Define $\mathbb{T}^{k,n}(\mathcal{P}_x)$ as the measure obtained from \mathcal{P}_x as follows. Conditional on the atoms $a_1 < a_2 < \dots$ of \mathcal{P}_x , we remove independently each of the atoms with respective probabilities

$$1 - \max_{z \in (t\frac{k}{n}, t\frac{k+1}{n}]} c(z + a_1), 1 - \max_{z \in (t\frac{k}{n}, t\frac{k+1}{n}]} c(z + a_2) \dots$$

and leave other atoms unchanged. Note that the thinning procedure is now independent of the starting time σ_x . Further, if $\sigma_x \in (t\frac{k}{n}, t\frac{k+1}{n}]$, the point measure $\mathbb{T}^{k,n}(\mathcal{P}_x)$ dominates $\bar{\mathcal{P}}_x$.

We decompose the births on $(0, t]$ into two parts: individuals stemming from the root \emptyset and a second part from subsequent births. Using the fact that for every individual x , the (un-suppressed) random measure \mathcal{P}_x is independent of its birth time σ_x (see second equality below), and setting $M(t) := \int_0^t \int_0^\infty g(a)\beta(a+u)c(u)dadu$, we get

$$\begin{aligned} B(t) &= \sum_{k=0}^{n-1} \sum_x \mathbb{E} \left(\mathbb{1} \left(\sigma_x \in \left(t\frac{k}{n}, t\frac{k+1}{n} \right] \right) \int_{[0, t-\sigma_x]} \bar{\mathcal{P}}_x(da) \right) + M(t) \\ &\leq \sum_{k=0}^{n-1} \sum_x \mathbb{E} \left(\mathbb{1} \left(\sigma_x \in \left(t\frac{k}{n}, t\frac{k+1}{n} \right] \right) \int_{[0, t-t\frac{k}{n}]} \mathbb{T}^{k,n}(\mathcal{P}_x)(da) \right) + M(t) \\ &= \sum_{k=0}^{n-1} \sum_x \mathbb{E} \left(\mathbb{1} \left(\sigma_x \in \left(t\frac{k}{n}, t\frac{k+1}{n} \right] \right) \right) \mathbb{E} \left(\int_{[0, t-t\frac{k}{n}]} \mathbb{T}^{k,n}(\mathcal{P})(da) \right) + M(t) \\ &= \sum_{k=0}^{n-1} \mathbb{E} \left(\sum_x \mathbb{1} \left(\sigma_x \in \left(t\frac{k}{n}, t\frac{k+1}{n} \right] \right) \right) \mathbb{E} \left(\int_{[0, t-t\frac{k}{n}]} \mathbb{T}^{k,n}(\mathcal{P})(da) \right) + M(t) \\ &= \sum_{k=0}^{n-1} \left(B\left(t\frac{k+1}{n}\right) - B\left(t\frac{k}{n}\right) \right) \mathbb{E} \left(\int_{[0, t-t\frac{k}{n}]} \mathbb{T}^{k,n}(\mathcal{P})(da) \right) + M(t) \\ &= \sum_{k=0}^{n-1} \left(B\left(t\frac{k+1}{n}\right) - B\left(t\frac{k}{n}\right) \right) \int_{[0, t-t\frac{k}{n}]} c^{k,n}(u)\beta(u)du + M(t). \end{aligned}$$

with $c^{k,n}(y) = \max_{v \in (t\frac{k}{n}, t\frac{k+1}{n}]} c(y+v)$. In particular, if $tk/n \rightarrow x$, and $x+y$ is a continuity point of c , we have $c^{k,n}(y) \rightarrow c(x+y)$. We will pass to the limit $n \rightarrow \infty$ in the latter inequality. Recall that c is bounded (and valued in $[0, 1]$) and that c is right-continuous. The first term on the RHS can be written under the form

$$\sum_{k=0}^{n-1} \left(B\left(t\frac{k+1}{n}\right) - B\left(t\frac{k}{n}\right) \right) \int_0^{t-[x]_n} c^{k,n}(u)\beta(u)du = \int_0^t f^n(x)dB(x),$$

where

$$f^{(n)}(x) = \int_0^{t-[x]_n} \sup_{v \in ([x]_n, [x]_n + \frac{t}{n})} c(v+u)\beta(u)du \quad \text{and} \quad [x]_n = \frac{t}{n} \lfloor nx/t \rfloor.$$

We will now apply twice the Bounded Convergence Theorem. On the one hand, for a fixed value of x , as $n \rightarrow \infty$

$$\mathbb{1}_{[0, t - [x]_n]}(u) \sup_{v \in ([x]_n, [x]_n + \frac{t}{n})} c(v + u)\beta(u) \rightarrow \mathbb{1}_{[0, t - x]}(u)c(x + u)\beta(u) \quad \text{Lebesgue a.e.}$$

Further, the latter term (i.e., the integrand in the integral defining f^n) is uniformly bounded by β and $\int_0^\infty \beta(u)du < \infty$. A first application of the Bounded Convergence Theorem implies that for every x , as $n \rightarrow \infty$

$$f^n(x) \rightarrow \int_0^{t-x} c(x + u)\beta(u)du.$$

On the other hand, the uniform bound, $f^n(x) \leq R_0 = \int_0^\infty \beta(u)du$ for all x, n , allows us to again apply the Bounded Convergence Theorem, so we get

$$B(t) \leq \int_0^t b(x)dx \int_{[0, t-x]} c(x + u)\beta(u)du + \int_0^t \int_0^\infty g(a)\beta(a + u)c(u)dadu.$$

By an analog argument, one can establish the same lower bound and strengthen the latter inequality into an equality. After a simple change of variable and interchanging the order of integration, this yields

$$B(t) = \int_0^t c(v) \int_0^v \beta(v - x)b(x)dx dv + \int_0^t \int_0^\infty g(a)\beta(a + u)c(u)dadu.$$

Finally, differentiating with respect to t yields the desired result. \square

Corollary 5 (Forward Feynman-Kac formula). *For every $t \geq 0$, define*

$$\bar{\mu}_t(da \times \{i\}) := n(t, a) \times \mathbb{P}(X(a) = i)da,$$

where n is the unique $\mathcal{L}^{1,loc}$ weak solution to the McKendrick-von Foerster PDE with initial condition g . Then

$$\bar{\mu}_t(da \times \{i\}) = \mathbb{E} \left(\sum_x 1_{\sigma_x < t} \delta_{(t - \sigma_x, X_x(t - \sigma_x))}(da \times \{i\}) \right) \quad (12)$$

where the expected value is taken with respect to a CMJ process starting with one individual with infection and life-process distributed according to the shifted law $\tilde{\mathcal{L}}_g$.

Proof. Define

$$\bar{\mu}'_t(da \times \{i\}) := \mathbb{E} \left(\sum_x 1_{\sigma_x < t} \delta_{(t - \sigma_x, X_x(t - \sigma_x))}(da \times \{i\}) \right)$$

We need to check that $\bar{\mu}'_t = \bar{\mu}_t$ on the space of finite measures. Let F be a measurable, non-negative, bounded, continuous function on $\mathbb{R} \times \mathbb{R} \times \mathcal{S}$ with compact support on $\mathbb{R}_+ \times \mathbb{R}_+ \times \mathcal{S}$. As in the previous lemma, we have

$$\begin{aligned} \int F(s, a, i) \bar{\mu}'_s(da, di) ds &= \sum_{x \neq 0} \mathbb{E} \left(\int F(s, s - \sigma_x, X_x(s - \sigma_x)) \mathbb{1}(\sigma_x < s) ds \right) \\ &\quad + \int_0^\infty \int_0^\infty \mathbb{E}(F(t, t + a, X(t + a))) g(a) dadt. \end{aligned}$$

Let (I) be the first term on the RHS. For every $n \in \mathbb{N}^*$

$$\begin{aligned}
(I) &= \sum_{k \geq 0} \sum_x \mathbb{E} \left(\int F(s, s - \sigma_x, X_x(s - \sigma_x)) \mathbb{1}(\sigma_x > s, \sigma_x \in (\frac{k}{n}, \frac{k+1}{n}]) ds \right) \\
&\leq \sum_{k \geq 0} \sum_x \mathbb{E} \left(\int_0^s \max_{u \in (\frac{k}{n}, \frac{k+1}{n}]} F(s, s - u, X_x(s - u)) \mathbb{1}(\sigma_x \in (\frac{k}{n}, \frac{k+1}{n}]) ds \right) \\
&= \sum_{k \geq 0} \sum_x \int_0^s \mathbb{E} \left(\max_{u \in (\frac{k}{n}, \frac{k+1}{n}]} F(s, s - u, X(s - u)) \right) \mathbb{P} \left(\sigma_x \in (\frac{k}{n}, \frac{k+1}{n}]) ds \right) \\
&= \sum_{k \geq 0} \int_0^s \mathbb{E} \left(\max_{u \in (\frac{k}{n}, \frac{k+1}{n}]} F(s, s - u, X(s - u)) \right) \left(B(\frac{k+1}{n}) - B(\frac{k}{n}) \right) ds
\end{aligned}$$

By reasoning along the same lines as in Lemma 4 (i.e., applying the Bounded Convergence Theorem several times) and using the almost sure continuity at every fixed time of the process X , one can show that the RHS converges to

$$\int_{s=0}^{\infty} \int_{u=0}^s \mathbb{E} \left(F(s, s - u, X(s - u)) \right) b(u) du ds$$

as $n \rightarrow \infty$ and thus

$$\begin{aligned}
\int F(s, a, i) \bar{\mu}'_s(da, di) ds &\leq \int_{s=0}^{\infty} \int_{u=0}^s \mathbb{E} \left(F(s, s - u, X(s - u)) \right) b(u) du ds \\
&\quad + \int_0^{\infty} \int_0^{\infty} \mathbb{E} (F(t, t + a, X(t + a))) g(a) dt.
\end{aligned}$$

By a similar argument, the inequality can be strengthened into an equality. Moreover we have

$$\begin{aligned}
\int F(s, a, i) \bar{\mu}_t(da, di) ds &= \int F(s, a, i) n(t, a) \mathbb{P}(X(a) \in di) da ds \\
&= \int_0^a \int F(s, a, i) b(s - a) \mathbb{P}(X(a) \in di) da ds + \int_a^{\infty} \int F(s, a, i) g(a - s) \mathbb{P}(X(a) \in di) da ds
\end{aligned}$$

so that

$$\int F(s, a, i) \bar{\mu}_t(da, di) = \int F(s, a, i) \bar{\mu}'_t(da, di).$$

Now take $F(s, a, i) = h(s)f(a, i)$ with h measurable, bounded, compact support on \mathbb{R}_+ and f bounded continuous. We get

$$\int h(s) \langle \bar{\mu}_s, f \rangle ds = \int h(s) \langle \bar{\mu}'_s, f \rangle ds.$$

On the other hand it is easy to check that the two functions $s \rightarrow \langle \bar{\mu}_s, f \rangle$ and $s \rightarrow \langle \bar{\mu}'_s, f \rangle$ are both continuous. As a consequence, we have $\langle \bar{\mu}_s, f \rangle = \langle \bar{\mu}'_s, f \rangle$ for every test function f , concluding the proof. \square

2.4 Dual CMJ process and backward Feynman-Kac formula

We end this section by making a connection between a dual process – interpreted as an *ancestral process* – and the (PDE) method of characteristics. In addition, this approach provides a probabilistic proof of uniqueness for the PDE.

Let \mathcal{M} be any random point measure with intensity measure $\tau(du)$. Fix $a, T > 0$. We now construct a dual process using the measure \mathcal{M} , which can be seen as a generalized Bellman-Harris branching process (individuals have a finite lifetimes, births only occur upon death). Let us first describe the process with no suppression (i.e., $c = 1$).

- Start with a single particle at time $t = 0$. Assume that the residual lifetime of this original particle is a , so that this particle dies out at time a .
- As in a Bellman-Harris process, the number of offspring of an individual and their lifetime durations are independent of the parent's characteristics.
- Upon death, each individual x is endowed with an independent copy \mathcal{M}_x of \mathcal{M} : the number of offspring of x is given by the number of atoms of \mathcal{M}_x and their lifetime durations are given by the positions of the atoms in \mathcal{M}_x .

The dual process with suppression $c \neq 1$ can be coupled with the case $c = 1$. Given a realization of the process, if a branching occurs at time t , the children are killed independently with probability $c(T - t)$. (Note that as in the original CMJ process, suppression translates into trimming the dual tree.)

Remark 4. *We note that there are as many dual processes as there are point processes with intensity measure τ . Here are a few natural choices:*

1. $\mathcal{M} = \mathcal{P}$.
2. *Let \mathcal{M} be a Poisson Point Process with intensity measure $\tau(du)$. In this particular case, the dual process is a Bellman-Harris branching process (i.e., the offspring lifetime durations are independent conditional on offspring number). We note that $\tau(du)$ appears naturally when considering the ancestral spine of a critical CMJ, see e.g. [28]. The measure τ can be obtained by size-biasing \mathcal{P} (i.e. biasing by the total mass of \mathcal{P}) and then recording the age of the individual at a uniformly chosen birth event.*

Let $(Y_t; t \geq 0)$ be the stochastic process valued in $\cup_{n \in \mathbb{N}} \mathbb{R}_+^n$ recording the residual lifetimes at time t listed in increasing order, i.e. if $Y_t = (Y_t^{(1)}, \dots, Y_t^{(n)})$ there are n particles alive at time t and $Y_t^{(k)}$ is the residual life-time of the k^{th} -individual with $Y_t^{(1)} < \dots < Y_t^{(n)}$. (We assumed that τ has a density so that the residual lifetimes are distinct a.s.). In particular, the particle labelled 1 at any given time t will be the first to expire, and at death time $t + Y_t^{(1)}$ a random number of children is produced. We let $\dim(Y_T)$ denote the number of particles alive at time t , i.e., the dimension of the vector Y_t .

Finally, we will say that n is a right-continuous version to the McKendrick-von Foerster equation, if n is a $\mathcal{L}^{1,loc}$ weak solution and for every $T, x \geq 0$ the function $s \rightarrow n(T-s, x-s)$ is right-continuous on $[0, x]$.

Proposition 6 (Backward Feynman-Kac formula). *Assume that the suppression function $(c(t); t \geq 0)$ is right-continuous. Then there is a unique right-continuous solution to the McKendrick-von Foerster equation, and for every $a, T \geq 0$*

$$n(T, a) = \widehat{\mathbb{E}}_a \left(\sum_{i \leq \dim(Y_T)} g(Y_T^{(i)}) \right) \quad (13)$$

where $\widehat{\mathbb{E}}_a$ is the distribution of the process $(Y_t; t \geq 0)$ starting with an individual with residual lifetime a .

Proof. We first assume that there exists a right-continuous solution to the PDE. Let $t_1 < \dots < t_k < \dots$ be the successive branching times of the dual branching process. Since τ has a density, there is a single branching particle at the successive branching times t_1, \dots . Define the càdlàg process

$$Z_s := \sum_{i \leq \dim(Y_s)} n(T - s, Y_s^{(i)})$$

See also Figure 2.4 for a pictorial representation of the process. It is plain from the definition that n is preserved along the characteristics of the PDE, i.e., that for every x the function $s \rightarrow n(T - s, x - s)$ remains constant on $[0, x)$. As a consequence, $(Z_s, s \geq 0)$ remains constant on every interval $[t_n, t_{n+1})$, with the convention $t_0 = 0$. Define $z_n := Z_{t_n}$ the value of the process $(Z_t; t \geq 0)$ at the n -th branching time. Let $(\mathcal{F}_n, n \in \mathbb{N})$ be the filtration induced by the process $(z_n; n \in \mathbb{N})$. For every $n > 1$

$$\begin{aligned} \widehat{\mathbb{E}}_a(z_n \mid \mathcal{F}_{n-1}) &= \sum_{2 \leq i \leq \dim(z_n)} n(T - t_n, Y_{t_n}^{(i)}) + c(T - t_n) \int_0^\infty n(T - t_n, a) \tau(da) \\ &= \sum_{2 \leq i \leq \dim(z_n)} n(T - t_n, Y_{t_n}^{(i)}) + n(T - t_n, 0) \\ &= z_{n-1}, \end{aligned}$$

where the second equality follows from the spatial boundary of the McKendrick-von Foerster equation. As already mentioned, the process $(Z_s; s \geq 0)$ is constant between two branching times. As a consequence, $(Z_s; s \geq 0)$ is a martingale (w.r.t. its natural filtration) so for every $s \geq 0$,

$$n(T, a) = \widehat{\mathbb{E}}_a \left(\sum_{i \leq \dim(Y_s)} n(T - s, Y_s^{(i)}) \right).$$

Relation (13) follows by taking $s = T$ in the latter expression.

The proof ends by checking that when c is right-continuous, the RHS of (13) indeed is a right-continuous solution to the PDE. This elementary step is left to the interested reader. \square

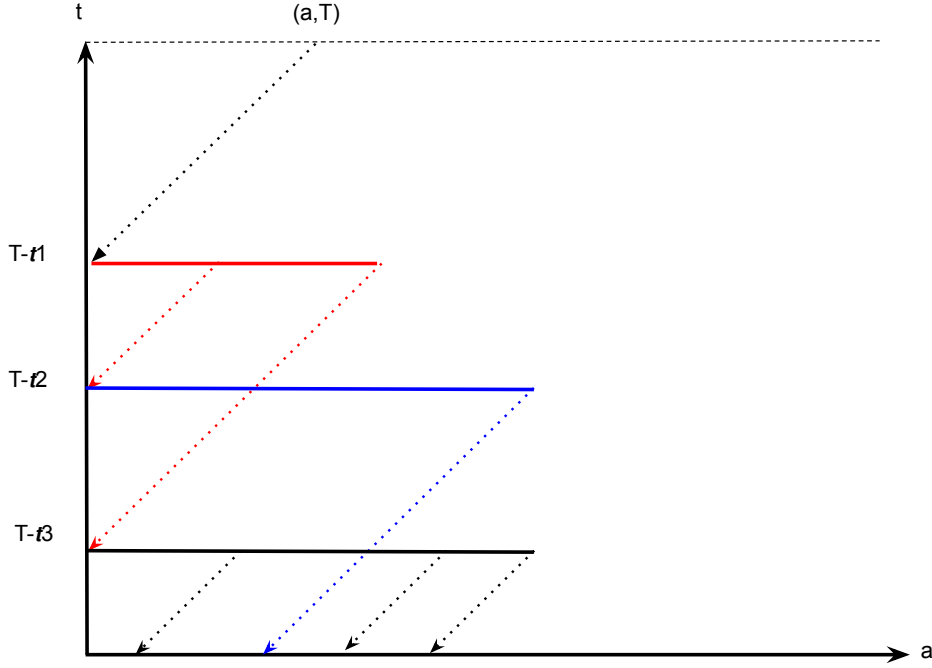


Figure 2: Graphical representation of the process $(Z_s; s \geq 0)$. We start with a single individual with residual lifetime a . In this picture, time flows downwards for the branching process. The residual lifetime of the initial individual decreases linearly until reaching 0 (this corresponds to time $T - t_1$ in our representation). At this time, the particle dies and produces 2 red particles. Residual lifetimes travel along the characteristics of the McKendrick-von Foerster PDE until reaching the spatial boundary condition $\{a = 0\}$ where a new branching occurs.

3 ~~Defn~~

Theorem 7 (N individuals). *Start with N individuals at time 0 with independent infection and life-processes distributed according to the initial shifted law $\tilde{\mathcal{L}}_g$. Define the empirical random measure for ages and types at time t*

$$\mu_t^N(\mathrm{d}a \times \{i\}) := \sum_x 1_{\sigma_x < t} \delta_{(t - \sigma_x, X_x(t - \sigma_x))}(\mathrm{d}a \times \{i\}). \quad (14)$$

As in Corollary 5, let

$$\bar{\mu}_t(\mathrm{d}a \times \{i\}) = n(t, a) \times \mathbb{P}(X(a) = i) \mathrm{d}a$$

where n is the unique $\mathcal{L}^{1, \text{loc}}$ weak solution to the McKendrick-von Foerster PDE with initial condition g . For every $t > 0$,

$$\frac{1}{N} \mu_t^N \xrightarrow[N \rightarrow \infty]{} \bar{\mu}_t \quad \text{a.s.}$$

where the convergence is meant in the weak topology.

Proof. We have

$$\mu_t^N(\mathrm{d}a \times \{i\}) = \frac{1}{N} \sum_{i=1}^N \mu_t^{1, (i)}(\mathrm{d}a \times \{i\}) \quad (15)$$

where $\{\mu_t^{1,(i)}\}$ are independent copies of μ_t^1 . Let f be an arbitrary measurable and bounded function on $\mathbb{R}_+ \times \mathcal{S}$. The L.L.N. combined with Corollary 5 implies that

$$\left\langle \frac{1}{N} \mu_t^N, f \right\rangle \rightarrow \langle \bar{\mu}_t, f \rangle \quad \text{a.s.}$$

which ends the proof. \square

In the following, we are motivated by modeling a situation where the infection is separated into two distinct phases. We start from a single individual.

- (Phase 1) We let the epidemic develop until a certain random time t_K . For instance, t_K could be the time at which the number of recorded deaths exceeds a large threshold K . We assume no suppression before t_K ;
- (Phase 2) We let the suppression function vary after time t_K , e.g., due to mitigation measures and/or behavioral changes (i.e., lockdown phase).

We will see in Theorem 8 below that the dynamics after time t_K converge to the same solution as in Theorem 7 but with an exponential initial age density ($g(x) = \alpha \exp(-\alpha x)$) and a (large) random number of initial infected individuals.

Let us now provide a more formal set-up. First ignore suppression and consider a plain CMJ process starting from one individual with shifted law $\tilde{\mathcal{L}}_g$. Let us now assume that the Malthusian parameter α of the CMJ process is strictly positive (supercritical assumption). We assume that g is chosen in such a way that there is a positive probability of non-extinction (to avoid trivialities).

Let $\mathcal{F}_t = \sigma(\{(\mathcal{P}_x, X_x) : x \in \bigcup_n \mathbb{N}^n, \sigma_x < t\})$ be the σ -field generated by the observation of the infection and life-cycle processes of the individuals born before time t (including the root \emptyset). Let $\{t_K\}$ be a sequence of stopping times (w.r.t. $(\mathcal{F}_t; t \geq 0)$) with $t_K \rightarrow \infty$ a.s. on the non-extinction event.

Now we assume that the suppression function $c^K \equiv c$ of the CMJ depends on K and that $c^K(t) := C(t - t_K)$, where $(C(t); t \in \mathbb{R})$ is a piecewise continuous function in $[0, 1]$ such that $C(t) = 1$ for all $t \leq 0$. Finally, $\mu_t^{t_K}$ is again the empirical measure of ages and types (as defined in (14)) w.r.t. the suppression function c^K .

Example 1. Take

$$t_K = \inf\{t > 0 : \#\{x \in \bigcup_n \mathbb{N}^n : \sigma_x < t, X_x(t - \sigma_x) = D\} \geq K\},$$

i.e., t_K is the first time that the accumulated number of deaths reaches level K .

Further take $C(t) = 1$ if $t \leq 0$ and $C(t) = r < 1$ if $t > 0$. This corresponds to a lockdown strategy where transmission is reduced by a factor r upon reaching K deaths.

Theorem 8 (One individual). *Conditional on non-extinction*

- There exists a r.v. W_∞ such that $W_\infty > 0$ a.s. and

$$\sum_x \mathbb{1}(0 < \sigma_x < t_K) \exp(-\alpha t_K) \xrightarrow[t_K \rightarrow \infty]{} W_\infty \quad \text{a.s. and in } L^1$$

- Fix $t \geq 0$. We have

$$\exp(-\alpha t_K) \mu_{t_K+t}^{t_K} \xrightarrow[t_K \rightarrow \infty]{} W_\infty \bar{\mu}_t \quad \text{in probability,}$$

where the convergence is meant in the weak topology, and

$$\bar{\mu}_t(da \times \{i\}) = n(t, a) \times \mathbb{P}(X(a) = i) da$$

with n the unique $\mathcal{L}^{1, \text{loc}}$ weak solution to the McKendrick-von Foerster PDE with initial condition $g(a) = \alpha \exp(-\alpha a)$ and suppression function $(C(t); t \geq 0)$.

Proof. We recall some basic facts about the method of random characteristics. We consider a plain CMJ with no death (no suppression function, no types). Every individual is characterized by an independent pair of random variables (\mathcal{P}, χ) . As before, \mathcal{P} is the infection measure recording the times of secondary infections. Now χ is a general stochastic process indexed by the age of the individual called a random characteristic with the convention $\chi(-a) = 0$ for $a \geq 0$. In great generality, \mathcal{P} and χ may exhibit a non-trivial correlation. Define

$$Z^\chi(T) = \sum_x \chi_x(T - \sigma_x)$$

the branching process counted by the random characteristic χ at time T . We now recall one of the main results of Jagers and Nerman [5] (see also Theorem 5, Appendix A in [6]). On top of all the assumptions above, we make the two following extra assumptions

- (a) There exists $\alpha' < \alpha$ such that

$$\mathbb{E} \left(\sup_{T \geq 0} \exp(-\alpha' T) \chi(T) \right) < \infty. \quad (16)$$

- (b) $T \rightarrow \mathbb{E}(\chi(T))$ is continuous a.e. with respect to the Lebesgue measure.

Then there exists a positive r.v. W_∞ (independent of the choice of χ) such that conditional on non-extinction

$$Z^\chi(T) \exp(-\alpha T) \rightarrow W_\infty \int_0^\infty \alpha \exp(-\alpha t) \mathbb{E}(\chi(t)) dt \quad \text{a.s. and in } L^1(dx) \text{ as } T \rightarrow \infty.$$

(Note that the L_1 convergence holds thanks to the $x \log(x)$ condition (9).)

To illustrate the method, we recall that if we take $\chi(T) = \mathbb{1}_{\mathbb{R}_+}(T)$ then $Z^\chi(T)$ coincides with $B(T)$, the total number of births before time T . For this particular choice of (deterministic) characteristic, the two properties above are immediately satisfied (recall that $\alpha > 0$), so that conditional on non-extinction

$$\sum_x \mathbb{1}(0 < \sigma_x < u) \exp(-\alpha u) \rightarrow W_\infty \quad \text{a.s. and in } L^1(dx) \text{ as } u \rightarrow \infty. \quad (17)$$

The a.s. convergence ensures that the first item of our theorem is satisfied.

Next, the second part of the theorem requires a choice of characteristic, called ‘general characteristic’, that depends on the descendance of each extant individual at time t_K . Because we need to prove an a.s. convergence result, whereas limit theorems on branching processes counted with general characteristics only hold in distribution, we have to design

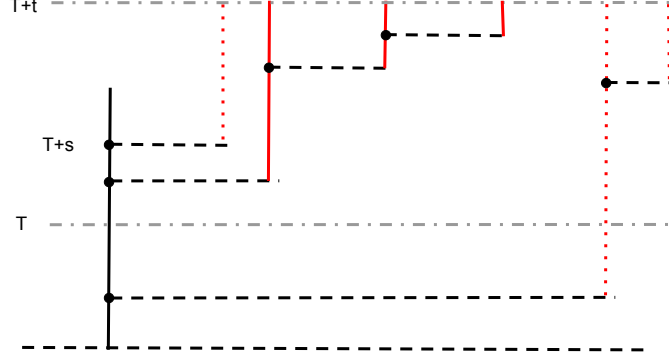


Figure 3: The individual x with characteristic (\mathcal{P}_x, X_x) under consideration is represented by a black segment. We graft independent (\mathcal{P}^*, X^*) -CMJ processes with suppression function $t \mapsto C(t - T)$ to the atoms of \mathcal{P}_x occurring at time $T + s$, independently with probability $C(s)$ if $s \geq 0$ and 0 if $s < 0$. We ignore all other atoms and their descendances (lower dotted red tree $s < 0$, upper dotted tree $s > 0$).

by hand an individual characteristic that has the same distribution as the requested general characteristic.

In order to define our next random characteristics, we start with some definition. Let (\mathcal{P}^*, X^*) be a pair of infection and life-cycle processes (that may or may not be identical to (\mathcal{P}, X) in distribution). One can construct a collection $(\mathcal{Z}^{(\Delta)}; \Delta \geq 0)$ of (\mathcal{P}^*, X^*) -CMJ processes starting at respective times Δ and with a suppression mechanism C , i.e.,

- $\mathcal{Z}^{(\Delta)}$ is a (\mathcal{P}^*, X^*) -CMJ process *starting at time* Δ with one progenitor.
- The suppression function applied to infection events is C .
- The previous rule applies at time $t = \Delta$, that is, $\mathcal{Z}^{(\Delta)}$ is identically empty with probability $1 - C(\Delta)$.

For any $t \geq \Delta$, we let $\nu^{(\Delta)}(t)$ denote the empirical measure for ages and types of $\mathcal{Z}^{(\Delta)}(t)$. Finally, we define $\{(\nu_i^{(\Delta)}; \Delta \geq 0)\}_{i \in \mathbb{N}^*}$ as the collection made of independent copies of the collection $(\nu^{(\Delta)}; \Delta \geq 0)$.

We are now ready to construct our random characteristics by enlarging the initial CMJ process in the following way. Fix $t \in \mathbb{R}_+$ and f a bounded non-negative continuous function on $\mathbb{R} \times \mathcal{S}$ with compact support in $\mathbb{R}_+ \times \mathcal{S}$. Consider a typical individual \emptyset , with infection and life processes (\mathcal{P}, X) . Denote by (r_i) the atoms of \mathcal{P} listed in increasing order. For any $T \geq 0$, define the individual random characteristic $\chi^{(t,f)}(T)$, by

$$\chi^{(t,f)}(T) := f(T + t, X(T + t)) + \sum_{i: r_i \in \mathcal{P} \cap [T, T+t]} \left\langle \nu_i^{(r_i - T)}(t), f \right\rangle,$$

See Figure 3 for a intuitive constructing of the random characteristics.

From now on, we assume that (\mathcal{P}^*, X^*) is identical in law to (\mathcal{P}, X) , which implies the following two crucial facts.

- (i) $\mathbb{E}(\int_0^\infty \chi^{(t,f)}(a)g(a)da) = \langle \bar{\mu}_t, f \rangle$ where $\bar{\mu}_t$ is defined as in Corollary 5 with initial condition g and suppression function C .
- (ii) Let us now count our branching process by its random characteristic

$$Z^{\chi^{(t,f)}}(T) = \sum_x \chi_x^{(t,f)}(T - \sigma_x).$$

Since t_K is a stopping time with respect to the filtration $(\mathcal{F}_t; t \geq 0)$, the branching property implies that $Z^{\chi^{(t,f)}}(t_K)$ is identical in distribution to $\langle \mu_{t_K+t}^{t_K}, f \rangle$ where we remember that $\mu_t^{t_K}$ is the empirical measure w.r.t. the CMJ process with suppression function $c^K : t \mapsto C(t - t_K)$.

In order to apply the aforementioned result of Jagers and Nerman, we need to check that condition (a), (b) above are satisfied. Condition (b) easily follows from the fact that τ has a density. We now check the first condition. Consider a (\mathcal{P}, X) -CMJ process, assuming that the initial individual is un-shifted. For every s , let $v_s(da \times \{i\})$ the empirical measure of ages and types at time s . We assumed f to be non-negative and thus

$$\mathbb{E}\left(\sup_{s \in [0,t]} \langle v_s, f \rangle\right) \leq \|f\|_\infty B(t).$$

Let $a_1 < a_2 < \dots$ be the atoms of \mathcal{P} between T and $T + t$. The random characteristic under consideration is obtained by attaching independent (suppressed) CMJ processes between T and $T + t$ to the a_i 's and by summing up the respective empirical measures at time $T + t - a_i$. By construction, $T \leq T + t - a_i \leq T + t$ so that

$$\begin{aligned} \mathbb{E}\left(\sup_{T \geq 0} \exp(-\alpha' T) \chi(T)\right) &\leq \mathbb{E}\left(\sup_{s \in [0,t]} \langle v_s, f \rangle\right) \mathbb{E}\left(\sup_{T \geq 0} \exp(-\alpha' T) \int_T^{T+t} \mathcal{P}(du)\right) \\ &= \|f\|_\infty B(t) \mathbb{E}\left(\sup_{T \geq 0} \exp(-\alpha' T) \int_T^{T+t} \mathcal{P}(du)\right) \\ &\leq R_0 B(t) \|f\|_\infty. \end{aligned}$$

This shows that property (a) is satisfied for any $0 \leq \alpha' < \alpha$. This shows that as $v \rightarrow \infty$, conditional on non-extinction

$$Z^{\chi^{(t,f)}}(v) \exp(-\alpha v) \rightarrow W_\infty \mathbb{E}\left(\int_0^\infty \alpha \exp(-\alpha u) \chi^{(t,f)}(u)\right) \quad \text{a.s.}$$

As already pointed out in (i),

$$\mathbb{E}\left(\int_0^\infty \alpha \exp(-\alpha u) \chi^{(t,f)}(u) du\right) = \langle \bar{\mu}_t, f \rangle$$

where $\bar{\mu}_t$ is defined as in Corollary 5 with initial condition $\alpha \exp(-\alpha t)$ and suppression function $(C(t); t \geq 0)$. Since the latter convergence is a.s. and $Z^{\chi^{(t,f)}}(t_K)$ is identical in law with $\langle \mu_{t_K+t}^{t_K}, f \rangle$ (see (ii) above), the result follows. \square

4 I6

4.1 Case study: the French COVID-19 epidemic

In this section, we illustrate how to use our framework to make inferences from macroscopic observables of the epidemic, e.g., incidence of positively tested patients, hospital or ICU (intensive care unit) admissions, deaths, *etc.* We show how to use those observables to extract the underlying age structure of the population, estimate model parameters and forecast the future of the epidemic.

We focused on a longitudinal case study in France. From March 18 2020, the French government has provided daily reports of the numbers of ICU and hospital admissions, of deaths, of discharged patients, and of occupied ICU and hospital beds. Moreover, several theoretical studies have already been conducted on the same dataset. This allowed us to fix the values of some crucial biological parameters that had already been estimated and to carry out a comparison with our method. We want to emphasize that the aim of this section is to provide a mathematical framework in which convergence results can be rigorously proved while remaining flexible enough for other applications. Our goal is not to provide new estimates of epidemiological parameters for France, as many robust estimates are already available. For instance we do not provide confidence intervals for our estimates, and neither do we conduct a sensibility analysis.

The remainder of the section is laid out as follows. In Section 4.2 we identify the mathematical quantities that impact the dynamics of the epidemic for large population sizes. Section 4.3 then presents the choice of distribution we made for these quantities and the parameters that need to be estimated. Finally, estimation of these parameters from the French incidence data is performed in Section 4.4. We start by fitting a simple model and then show how this model can be made more complex to account for more complex incidence data.

4.2 The model

As mentioned previously, the age structure of the population cannot be directly accessed. What is observed is a subset of the population with some characteristic of interest, for instance individuals that have been tested positively, deceased individuals or discharged patients. Recall that under the assumptions stated in Section 3, the number of individuals that are in a given state i at time t converges to

$$\int_0^\infty n(t, a) \mathbb{P}(X(a) = i) da,$$

where $(n(t, a))$ is the solution to the McKendrick-von Foerster equation. Note that the assumptions of Theorem 8 are in essence that the epidemic has been ongoing for a long enough time at the lockdown onset for the infected population to be large, which we assume to hold true for France as the number of infected individuals on March 16 2020 was on the order of tens of thousands of individuals.

The McKendrick-von Foerster equation is determined by two quantities: (i) the average infection measure τ defined in 2.1 and (ii) an initial condition, which is of the form

$$\forall a \geq 0, \quad n(0, a) = W \alpha e^{-\alpha a}$$

for some initial number of infected individuals W and a parameter α which corresponds to the exponential growth rate of the epidemic before the lockdown onset.

Therefore, using Theorem 8 to obtain a theoretical prediction for some observables under consideration requires the knowledge of:

1. The intensity measure τ of secondary infections;
2. The initial number of infected W and the parameter α ;
3. For each state i of interest the probability $\mathbb{P}(X(a) = i)$.

The next section exposes how we have parametrized these quantities.

4.3 Parametrization of the model

Average infection measure. Recall the definition of τ from Section 2.1. Let us further define

$$R_0 = \tau([0, \infty)), \quad \hat{\tau}(da) = \frac{\tau(da)}{\tau([0, \infty))},$$

so that τ can be expressed as

$$\tau(da) = R_0 \hat{\tau}(da).$$

The total mass of τ , R_0 , is the mean number of secondary infections induced by a single infected individual. Thus R_0 corresponds to the basic reproduction number of the epidemic, and we leave it as a parameter to infer. The epidemiological interpretation of the probability measure $\hat{\tau}$ is the following. Consider a large population of infected individuals. Then, as the size of that population goes to infinity, the distribution of the time between the infection of a uniformly sampled individual and the infection of its “parent” converges to $\hat{\tau}$. Therefore, $\hat{\tau}$ is the distribution of the so-called generation time of the epidemic, which has already been estimated in several previous studies. We used the estimation of [29], and assumed that $\hat{\tau}$ is a Weibull distribution, that is

$$\hat{\tau}(da) = \frac{k}{\lambda} \left(\frac{a}{\lambda}\right)^{k-1} e^{-(a/\lambda)^k} da, \quad (18)$$

where the values of the shape parameter k and scale parameter λ are recalled in Table 1.

Initial condition. The growth rate α is defined implicitly through equation (8). Moreover, we know that α corresponds to the exponential growth rate of *any* of the observables of the epidemic before the lockdown onset. We chose to estimate α from the cumulative number of deaths, which appeared to be more reliable than the number of positive tests as the number of tests that have been conducted in the early phase of the epidemic in France varied greatly. We simply estimated α using a linear regression on the logarithm of the number of deaths from March 7 to March 20, 2020. The estimated α as well as the corresponding R_0 pre-lockdown are shown in Table 1. The number of infected individuals at the time of lockdown was left as a parameter to infer.

Life-cycle. The last quantities that need to be defined are the one-dimensional marginals of the life-cycle process $(X(a); a \geq 0)$. From now on, we assume that the sequence of states visited by $(X(a); a \geq 0)$ is a Markov chain and that the sojourn times in each state is Gamma distributed.

More specifically, we suppose that we are given a global dispersion parameter $\gamma > 0$ and that for each state $i \in \mathcal{S}$, the time D_i spent in state i follows a Gamma distribution with expectation $t_i > 0$ and variance t_i/γ ,

- $\mathbb{E}(D_i) = t_i$
- $\text{Var}(D_i) = t_i/\gamma$

This assumption has the following consequence. Let i_1, \dots, i_k be a possible sequence of states of $(X(a); a \geq 0)$, and denote by T_{i_1}, \dots, T_{i_k} the respective entrance times in these states. Then conditional on $(X(a); a \geq 0)$ successively visiting the states i_1, \dots, i_k in this order, we have

$$(T_{i_1}, \dots, T_{i_k}) \sim (0, Y_{t_1}, \dots, Y_{t_1 + \dots + t_{k-1}})$$

where $(Y_t)_{t \geq 0}$ is a Gamma process such that

$$Y_t \sim \frac{\gamma^{\gamma t}}{\Gamma(\gamma t)} a^{\gamma t - 1} e^{-\gamma a} da.$$

Another advantage of this parametrization is that the 1d marginals of $(X(a); a \geq 0)$ can be computed efficiently, while only requiring one parameter for each state of interest, and a global dispersion parameter.

4.4 Fitting the model to incidence data

In this section, we fit six time series of the French epidemic: the number of ICU and hospital admissions, the number of deaths, the number of occupied ICU and hospital beds and the number of discharged patients. We provide two examples of Markov chains that we use to fit these data. The first Markov chain is only used to fit the first three curves, that we will call *incidence curves*, i.e., the daily number of ICU admissions, of hospital admissions and of deaths. With the parametrization of the previous section, the predictions of our model for these time series only involves the delay between infection and death, ICU, or hospital admissions. We do not need to estimate the time between hospitalization and discharge, which makes the model and the inference procedure easier. Then we show how this model can be made more complex to fit the last three curves, that we call *prevalence curves*. All parameter estimations were realized using the data from March 18 to May 11, 2020. This time frame corresponds to the lockdown period in France.

Fitting incidence data. In order to fit the incidence curves, we considered the simplest model that can account for these three time series. The model is illustrated in Figure 4.

Upon infection, with probability $1 - p_{\text{hosp}}$, an individual develops a mild form of COVID-19 and is placed in state I , which encompasses all cases that do not require a hospitalization. With probability p_{hosp} the individual has a severe infection and is placed in state C . Individuals in state C are eventually hospitalized and moved to state H .

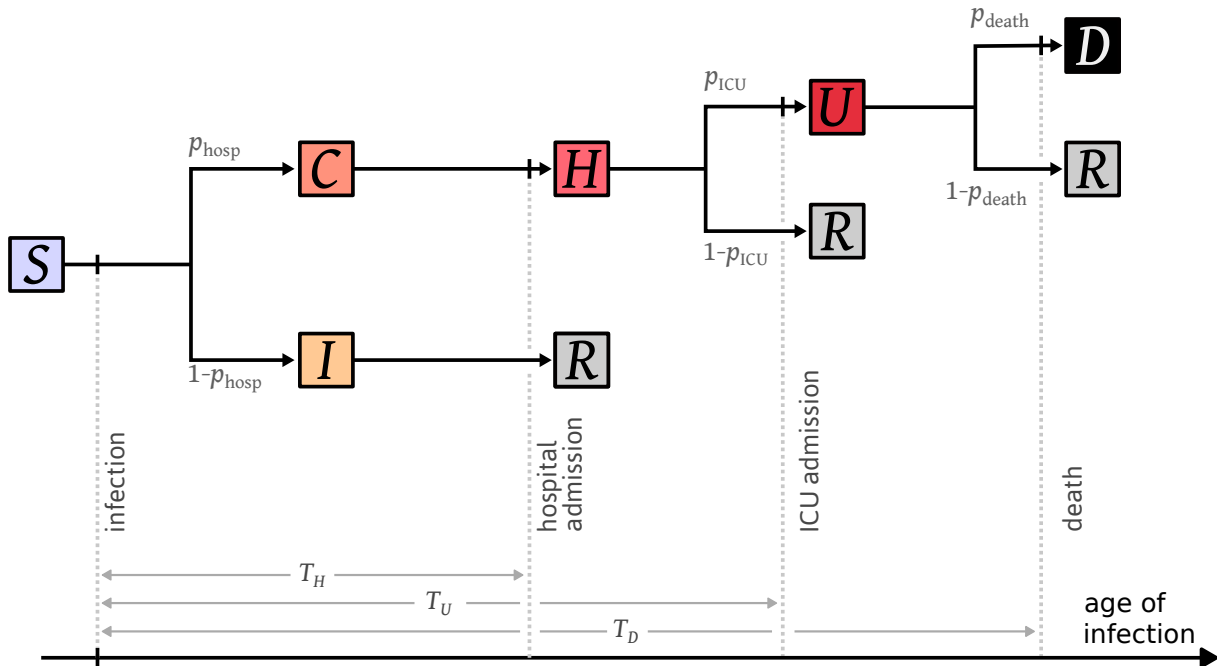


Figure 4: Illustration of the admission model.

Then, with probability p_{ICU} individuals in state H are admitted in ICU and move to state U . Otherwise they eventually recover and are discharged. Finally, individuals in state U die with probability p_{death} , or recover with probability $1 - p_{\text{death}}$. In this model, only individuals in ICU may die.

As we are fitting the number of individuals that enter a state, and not the number of individuals that are currently in that state, we only need to track the times T_H , T_U , and T_D elapsed between infection and hospital admission, ICU admission and death, respectively. We will refer to this model as the *admission model*.

Estimations for p_{hosp} , p_{ICU} and of death probability conditional on hospitalization (equal in our setting to $p_{\text{ICU}} \times p_{\text{death}}$) in France have already been conducted in [11]. We used these estimates and considered the values of p_{hosp} , p_{ICU} and p_{death} to be fixed. All other parameters were estimated using a maximum likelihood procedure which is described in Appendix A. The parameter estimations are provided in Table 2, and the corresponding predicted values for the time series under consideration are displayed in Figure 5. Overall, our simple model seems to match the observed data. Note however that the model overestimates the number of ICU admissions in the second part of the lockdown. This is likely due to a temporal reduction in the ICU admission probability which has been reported in [11].

Our estimation of the basic reproduction number during the lockdown period is $R_0 = 0.745$. This suggests that lockdown has reduced the basic reproduction number by a factor 0.23 compared to the beginning of the epidemic. Moreover, we estimated that 9.85×10^5 infections have occurred in France before March 17th. Both these values are in line with previous estimates for France [30, 11].

We did not impose that $T_H < T_U$ in the inference procedure. Interestingly we found that the data are best explained by assuming that the mean of T_H is 14.4 days, whereas the mean of T_U is 11.4 days. This indicates that the delay between infection and hospital

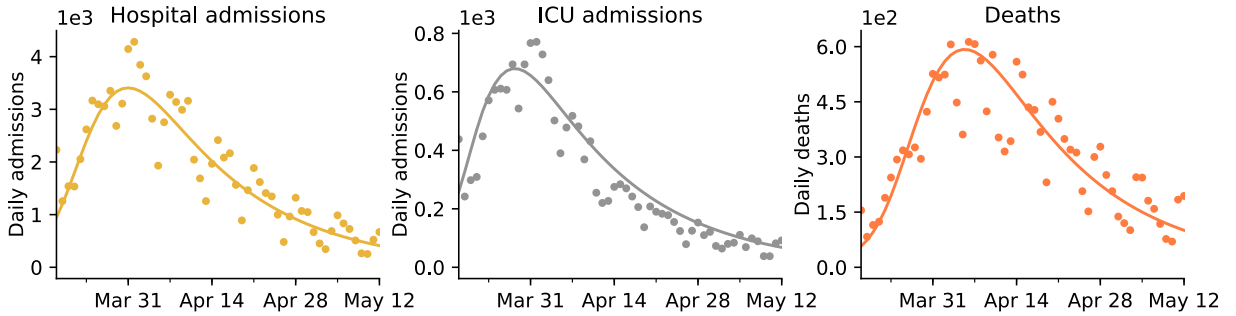


Figure 5: Best fit of the admission model. Solid line correspond to the number of hospital admissions, ICU admissions and deaths predicted by the admission model. The dots are the corresponding observed values.

Notation	Description	Value	Source
α	Pre-lockdown exponential growth rate	0.315	E
R_{pre}	Basic reproduction number before lockdown	3.25	E
k	Shape parameter of the generation time	2.83	[29]
λ	Scale parameter of the generation time	5.67	[29]

Table 1: Parameter values common to both models. In the “Source” column, “E” indicates that the parameter has been estimated in the present work.

admission is shorter for individuals that end up in ICU, compared to the average time between infection and hospitalization. Therefore it would be more appropriate to allow individuals to have an admission to hospital delay that is different depending on whether they will end up in ICU or not, modeling the fact that they have a more severe form of the disease. We estimated the mean of T_D , the time between infection and death, to be 18.6 days. This estimate is lower than but consistent with previous estimates based on the study of individual-case data [3, 31, 32].

Fitting prevalence data. A first attempt to fit the prevalence curves could be to keep the admission model of Figure 4 and to estimate the time between hospital admission and discharge using the observed number of occupied ICU, hospital beds, and discharged patients. However this only yields a poor fit of the data (see Appendix B). We identified two main reasons for this discrepancy. First, we assumed that all individuals are admitted to ICU prior to death. Using the probability estimated in [11] then yields that the probability of dying conditional on being in ICU is 0.953. This value is unrealistically high, and we need to assume that a fraction of hospital deaths occur without going through the ICU. Second, under the admission model, the delay between hospital admission and discharge is almost unimodal. However, the observed number of occupied hospital beds rises fast but falls slowly. Such a shape cannot be easily accounted for by a unimodal distribution for the time spent in hospital.

Taking into account the previous two points required us to make the model more com-

Notation	Description	Value	Source
R_0	Basic reproduction number during lockdown	0.745	E
W	Total number of infections before March 17 2020	9.85×10^5	E
p_{hosp}	Probability of being hospitalized	0.036	[11]
p_{ICU}	Probability of entering ICU conditional on being at the hospital	0.19	[11]
$p_{\text{ICU}} \cdot p_{\text{death}}$	Death probability conditional on being hospitalized	0.181	[11]
T_H	Delay between infection and hospital admission	14.4 days	E
T_U	Delay between infection and ICU admission	11.4 days	E
T_D	Delay between infection and death	18.6 days	E
γ	Scale parameter common to all Gamma distributions	0.463	E

Table 2: Inferred parameter set for the admission model. The values indicated for the durations correspond to the means of the Gamma distributions. In the ‘‘Source’’ column, ‘‘E’’ indicates that the parameter has been estimated in the current work.

plex. The resulting model, referred to as the *occupancy model*, is illustrated in Figure 6. We now consider that upon infection, individuals go to one of three states depending on the severity of their infection:

- The state C_u which gathers critical infections that lead to death or ICU admission. The probability of having a critical infection is denoted by p_{crit} .
- The state C_h which corresponds to severe infections that require a hospitalization but are not critical. Such infections occur with probability p_{sev} .
- The I state which consists of all mild infections that do not lead to a hospital admission, and occur with probability $1 - p_{\text{crit}} - p_{\text{sev}}$.

Individuals in state C_h are admitted to hospital after a duration D_{C_h} . Then, with probability p_{short} they are discharged after a duration D_{short} , while with probability $1 - p_{\text{short}}$ they are discharged after a duration D_{long} .

Critically infected individuals are admitted to hospital after a duration D_{C_u} . Upon arrival at hospital, they die immediately with probability d_{hosp} , or go to ICU after a duration D_{H_u} . Individuals in ICU die with probability d_{ICU} after a delay D_D . Otherwise they are discharged after a stay of length D_U .

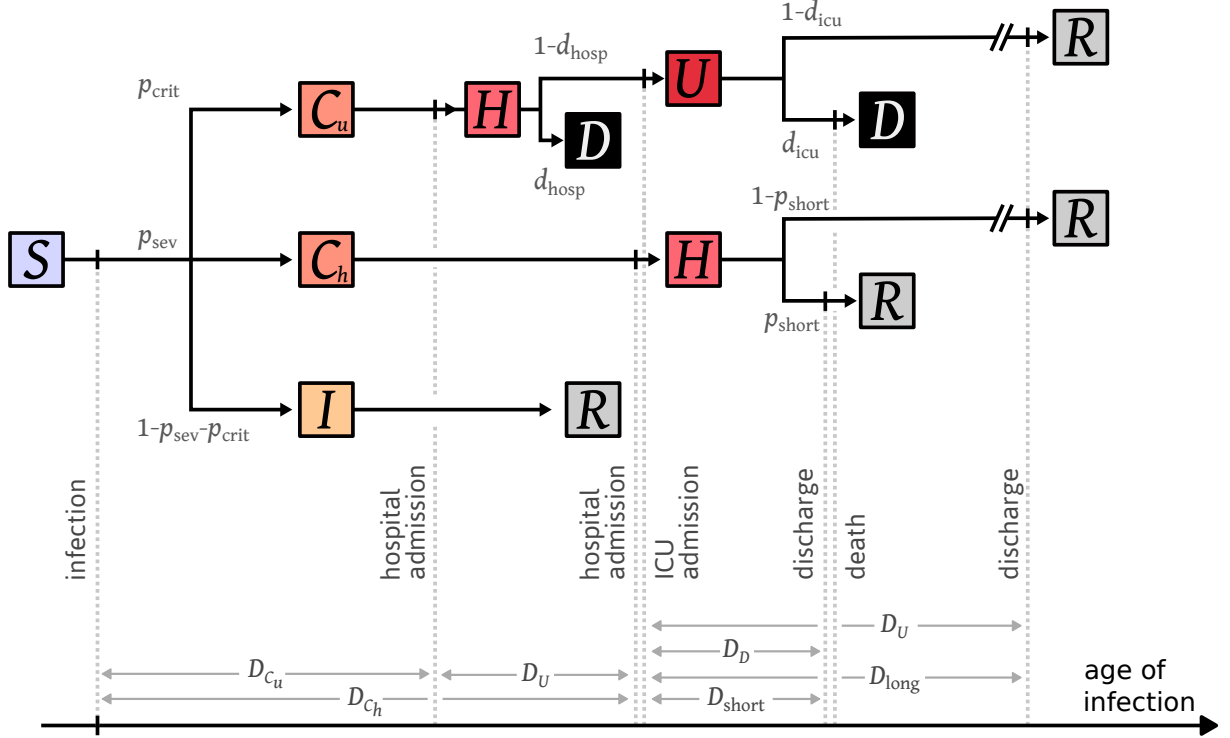


Figure 6: Illustration of the occupancy model

In our model, the probability of hospital admission is $p_{\text{crit}} + p_{\text{sev}}$, the probability of ICU admission is $p_{\text{crit}}(1 - d_{\text{hosp}})$ and that of death is $p_{\text{crit}}(d_{\text{hosp}} + (1 - d_{\text{hosp}})d_{\text{ICU}})$. We have fixed these three values to those estimated in [11], and we only had one remaining parameter out of 4 (p_{crit} , p_{sev} , d_{short} , d_{ICU}) to estimate from the data. We have fixed the time D_U to 1.5 days as estimated in [11]. All other parameters were estimated using the same likelihood method as previously, which is described in Section A. The estimated parameter set is shown in Table 3, while Figure 7 shows the best-fitting model.

The estimated parameters provide a good fit of the six observed time series. Again, the model has a tendency to overestimate the ICU admissions in the second part of the lockdown, which has the same interpretation as before.

Under the occupancy model, we estimated that $R_0 = 0.734$, and $W = 9.52 \times 10^5$. These estimates are extremely close to those made with the admission model. The estimated mean time between infection and death or hospital, ICU admission are respectively 19.5 days, 13.7 days and 12.5 days. Again we see that these estimates in the more complex model are consistent with those of the simple model. The mean recovery time from hospital is 19.4 days for severe infections, and 28.2 days for critical infections. This yields an overall mean recovery time of 20.0 days. Finally, we estimated that the death probability conditional on being in ICU is 0.709. This yields that in our model a fraction 0.256 of all deaths occur shortly after hospital admission. This result is consistent with [11] that estimated that a fraction 0.15 of all deaths occurred within the first day after hospital admission. However, it has been reported in [33] that the death probability of ICU patients is 0.23. Our estimated value is thus unrealistically high. This indicates that there is a fraction of hospital deaths that occur without any ICU admission, and not quickly after hospital admission, that our model is not accounting for.

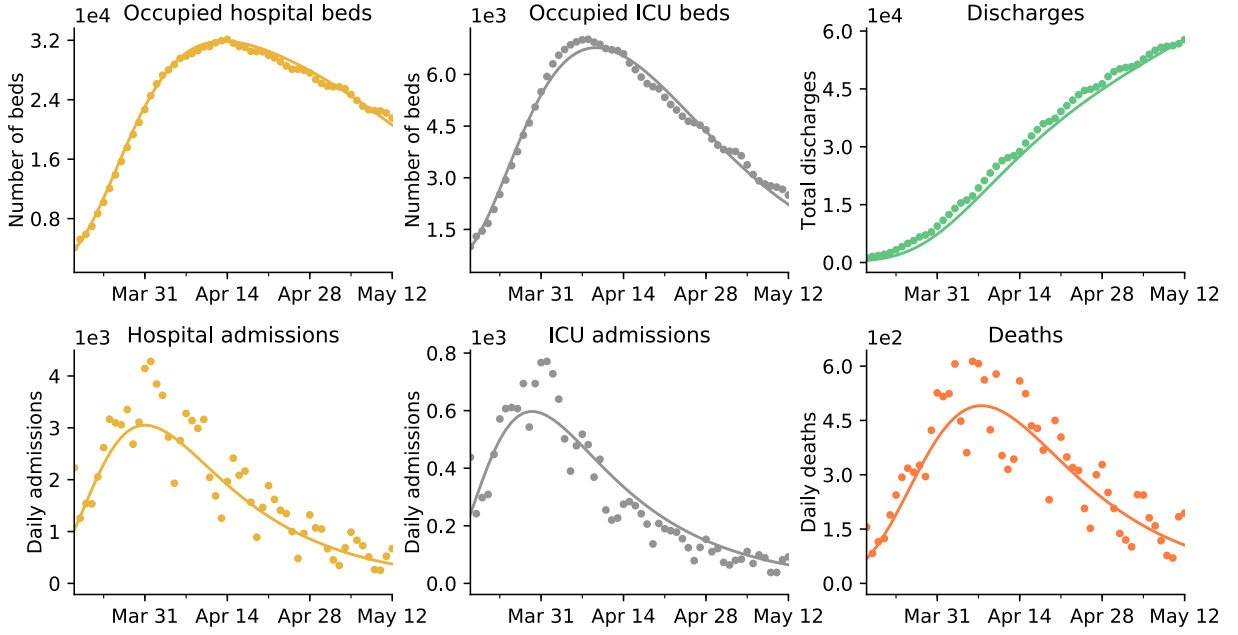


Figure 7: Best fit of the admission model. The solid lines correspond to the number of deaths, discharges, occupied ICU and hospital beds and ICU and hospital admissions predicted by the occupancy model. The dots are the corresponding observed values.

Our estimates, though they are not the key message of the present paper, can nevertheless draw attention to potential heterogeneities in the infected population. We estimated that the mean time between infection and ICU admission is shorter than that between infection and hospital admission. This suggests that the time between infection and severe symptom onset is shorter for critical infection, that lead to ICU admission, than for milder ones. Moreover, fitting the prevalence time series required to divide the hospital and death compartments in two subcompartments, indicating that the data are not well explained by a simple homogeneous model, as seen in Figure 8. Such heterogeneity could originate from underlying structuring variables, such as comorbidity or (real) age, that we are not accounting for. Many estimates of clinical features, such as the incubation period, are obtained from a pooled dataset that does not take heterogeneity in the population into account [34, 31, 35, 36, 37, 38, 14]. When estimating the total number of infected individuals using only a fraction of the detected cases, e.g., using the hospital admissions or deaths, it is interesting to keep in mind that the time periods estimated from pooled studies could be inaccurate for the fraction of infected individuals under consideration.

Acknowledgements. The authors thank the *Center for Interdisciplinary Research in Biology* (CIRB) for funding and the taskforce MODCOV19 of the INSMI (CNRS) for their technical/scientific support during the epidemic. P.C. has received funding from the European Union’s Horizon 2020 research and innovation program under the Marie Skłodowska-Curie grant agreement PolyPath 844369.

Notation	Description	Value	Source
R_0	Basic reproduction number during lockdown	0.734	E
W	Total number of infections before March 17 2020	9.52×10^5	E
$p_{\text{crit}} + p_{\text{sev}}$	Probability of being hospitalized	0.036	[11]
$\frac{p_{\text{crit}}(1-d_{\text{hosp}})}{p_{\text{crit}}+p_{\text{sev}}}$	Probability of entering ICU conditional on being at the hospital	0.19	[11]
$\frac{d_{\text{hosp}}+(1-d_{\text{hosp}})d_{\text{ICU}}}{1+p_{\text{sev}}/p_{\text{crit}}}$	Death probability conditional on being hospitalized	0.181	[11]
d_{ICU}	Probability of death conditional on being in ICU	0.709	E
p_{short}	Probability of a short stay at hospital	0.701	E
D_{C_h}	Delay between severe infection and hospital admission	14.5 days	E
D_{short}	Delay between hospital admission and quick discharge	7.36 days	E
D_{long}	Delay between hospital admission and slow discharge	47.5 days	E
D_{C_u}	Delay between critical infection and hospital admission	11.0 days	E
D_H	Delay between hospital admission and ICU admission	1.5 days	[11]
D_U	Delay between ICU admission and discharge	28.2 days	E
D_D	Delay between ICU admission and death	9.90 days	E
γ	Scale parameter common to all Gamma distributions	0.316	E

Table 3: Inferred parameter set for the occupancy model. The values indicated for the durations correspond to the means of the Gamma distributions. In the ‘‘Source’’ column, ‘‘E’’ indicates that the parameter has been estimated in the current work.

R

- [1] H. Krauss. *Zoonoses : infectious diseases transmissible from animals to humans*. ASM Press, 2003.
- [2] Dorothy H. Crawford. *Deadly companions: how microbes shaped our history*. Oxford University Press, second edition, 2018.
- [3] Joseph T. Wu, Kathy Leung, Mary Bushman, Nishant Kishore, Rene Niehus, Pablo M. de Salazar, Benjamin J. Cowling, Marc Lipsitch, and Gabriel M. Leung. Estimating clinical severity of COVID-19 from the transmission dynamics in Wuhan, China. *Nature Medicine*, 26(4):506–510, 2020.
- [4] Olle Nerman. On the convergence of supercritical general (C-M-J) branching processes. *Zeitschrift für Wahrscheinlichkeitstheorie und Verwandte Gebiete*, 57(3):365–395, 1981.
- [5] Peter Jagers and Olle Nerman. The growth and composition of branching populations. *Advances in Applied Probability*, 16(2):221–259, 1984.
- [6] Ziad Taïb. *Branching Processes and Neutral Evolution*, volume 93 of *Lecture Notes in Biomathematics*. Springer Berlin Heidelberg, Berlin, Heidelberg, 1992.
- [7] Tom Britton, Frank Ball, and Pieter Trapman. The disease-induced herd immunity level for COVID-19 is substantially lower than the classical herd immunity level. *arXiv preprint arXiv:2005.03085*, 2020.
- [8] Tom Britton. Epidemics in heterogeneous communities: estimation of R_0 and secure vaccination coverage. *Journal of the Royal Statistical Society: Series B (Statistical Methodology)*, 63(4):705–715, 2001.
- [9] Harry Cohn. Multitype finite mean supercritical age-dependent branching processes. *Journal of applied probability*, 26(2):398–403, 1989.
- [10] Jean-Jil Duchamps, Felix Foutel-Rodier, and Emmanuel Schertzer. *From individual-based epidemic models to McKendrick-von Foerster PDE's: the non-linear case*. In progress, 2020.
- [11] Henrik Salje, Cécile Tran Kiem, Noémie Lefrancq, Noémie Courtejoie, Paolo Bosetti, Juliette Paireau, Alessio Andronico, Nathanaël Hozé, Jehanne Richet, Claire-Lise Dubost, Yann Le Strat, Justin Lessler, Daniel Levy-Bruhl, Arnaud Fontanet, Lulla Opatowski, Pierre-Yves Boelle, and Simon Cauchemez. Estimating the burden of SARS-CoV-2 in France. *Science*, 369(6500):208–211, 2020.
- [12] Lionel Roques, Etienne K Klein, Julien Papaix, Antoine Sar, and Samuel Soubeyrand. Using early data to estimate the actual infection fatality ratio from COVID-19 in France. *Biology*, 9(5):97, 2020.
- [13] Theodoros Evgeniou, Mathilde Fekom, Anton Ovchinnikov, Raphael Porcher, Camille Pouchol, and Nicolas Vayatis. Epidemic models for personalised COVID-19 isolation and exit policies using clinical risk predictions. *medRxiv*, 2020.

- [14] Ramses Djidjou-Demasse, Yannis Michalakis, Marc Choisy, Micea T Sofonea, and Samuel Alizon. Optimal COVID-19 epidemic control until vaccine deployment. *medRxiv*, 2020.
- [15] Thomas Sellke. On the asymptotic distribution of the size of a stochastic epidemic. *Journal of Applied Probability*, 20(2):390–394, 1983.
- [16] Guodong Pang and Etienne Pardoux. Functional limit theorems for non-Markovian epidemic models. *arXiv preprint arXiv:2003.03249*, 2020.
- [17] Frank Ball. A unified approach to the distribution of total size and total area under the trajectory of infectives in epidemic models. *Advances in Applied Probability*, 18(2):289–310, 1986.
- [18] Andrew D Barbour. The duration of the closed stochastic epidemic. *Biometrika*, 62(2):477–482, 1975.
- [19] Peter Jagers. *Branching processes with biological applications*. Wiley, 1975.
- [20] Jie Yen Fan, Kais Hamza, Peter Jagers, and Fima Klebaner. Convergence of the age structure of general schemes of population processes. *Bernoulli*, 26(2):893–926, 2020.
- [21] Peter Jagers and Olle Nerman. Limit theorems for sums determined by branching and other exponentially growing processes. *Stochastic Processes and their Applications*, 17(1):47–71, 1984.
- [22] Peter Jagers and Fima C Klebaner. Population-size-dependent, age-structured branching processes linger around their carrying capacity. *Journal of Applied Probability*, 48(A):249–260, 2011.
- [23] Peter Jagers and Fima C Klebaner. Population-size-dependent and age-dependent branching processes. *Stochastic Processes and their Applications*, 87(2):235–254, 2000.
- [24] Kais Hamza, Peter Jagers, and Fima C Klebaner. The age structure of population-dependent general branching processes in environments with a high carrying capacity. *Proceedings of the Steklov Institute of Mathematics*, 282(1):90–105, 2013.
- [25] Viet Chi Tran. Large population limit and time behaviour of a stochastic particle model describing an age-structured population. *ESAIM: Probability and Statistics*, 12:345–386, 2008.
- [26] Regis Ferriere and Viet Chi Tran. Stochastic and deterministic models for age-structured populations with genetically variable traits. In *ESAIM: Proceedings*, volume 27, pages 289–310. EDP Sciences, 2009.
- [27] Peter Olofsson. The $x \log x$ condition for general branching processes. *Journal of applied probability*, 35(3):537–544, 1998.
- [28] Emmanuel Schertzer and Florian Simatos. Height and contour processes of Crump-Mode-Jagers forests (I): general distribution and scaling limits in the case of short edges. *Electronic Journal of Probability*, 23:43pp., 2018.

- [29] Luca Ferretti, Chris Wymant, Michelle Kendall, Lele Zhao, Anel Nurtay, Lucie Abeler-Dörner, Michael Parker, David Bonsall, and Christophe Fraser. Quantifying SARS-CoV-2 transmission suggests epidemic control with digital contact tracing. *Science*, 368(6491), 2020.
- [30] Mircea T. Sofonea, Bastien Reyné, Baptiste Elie, Ramsès Djidjou-Demasse, Christian Selinger, Yannis Michalakis, and Samuel Alizon. Epidemiological monitoring and control perspectives: application of a parsimonious modelling framework to the COVID-19 dynamics in France. *medRxiv*, 2020.
- [31] Natalie M. Linton, Tetsuro Kobayashi, Yichi Yang, Katsuma Hayashi, Andrei R. Akhmetzhanov, Sung-mok Jung, Baoyin Yuan, Ryo Kinoshita, and Hiroshi Nishiura. Incubation period and other epidemiological characteristics of 2019 novel coronavirus infections with right truncation: A statistical analysis of publicly available case data. *Journal of Clinical Medicine*, 9(2):538, 2020.
- [32] Robert Verity, Lucy C. Okell, Iliaria Dorigatti, Peter Winskill, Charles Whittaker, Natsuko Imai, Gina Cuomo-Dannenburg, Hayley Thompson, Patrick G. T. Walker, Han Fu, Amy Dighe, Jamie T. Griffin, Marc Baguelin, Sangeeta Bhatia, Adhiratha Boonyasiri, Anne Cori, Zulma Cucunubá, Rich FitzJohn, Katy Gaythorpe, Will Green, Arran Hamlet, Wes Hinsley, Daniel Laydon, Gemma Nedjati-Gilani, Steven Riley, Sabine van Elsland, Erik Volz, Haowei Wang, Yuanrong Wang, Xiaoyue Xi, Christl A. Donnelly, Azra C. Ghani, and Neil M. Ferguson. Estimates of the severity of coronavirus disease 2019: a model-based analysis. *The Lancet Infectious Diseases*, 20(6):669–677, 2020.
- [33] Santé Publique France. COVID-19 : point épidémiologique du 4 juin 2020, 2020.
- [34] Jantien A. Backer, Don Klinkenberg, and Jacco Wallinga. Incubation period of 2019 novel coronavirus (2019-nCoV) infections among travellers from Wuhan, China, 20-28 January 2020. *Eurosurveillance*, 25(5), 2020.
- [35] Stephen A Lauer, Kyra H Grantz, Qifang Bi, Forrest K Jones, Qulu Zheng, Hannah R Meredith, Andrew S Azman, Nicholas G Reich, and Justin Lessler. The incubation period of coronavirus disease 2019 (COVID-19) from publicly reported confirmed cases: Estimation and application. *Annals of internal medicine*, 172(9):577–582, 2020.
- [36] Lauren Tindale, Michelle Coombe, Jessica E Stockdale, Emma Garlock, Wing Yin Venus Lau, Manu Saraswat, Yen-Hsiang Brian Lee, Louxin Zhang, Dongxuan Chen, Jacco Wallinga, and Caroline Colijn. Transmission interval estimates suggest pre-symptomatic spread of COVID-19. *medRxiv*, page 2020.03.03.20029983, 2020.
- [37] Qifang Bi, Yongsheng Wu, Shujiang Mei, Chenfei Ye, Xuan Zou, Zhen Zhang, Xiaojian Liu, Lan Wei, Shaun A Truelove, Tong Zhang, Wei Gao, Cong Cheng, Xiujuan Tang, Xiaoliang Wu, Yu Wu, Binbin Sun, Suli Huang, Yu Sun, Juncen Zhang, Ting Ma, Justin Lessler, and Teijian Feng. Epidemiology and transmission of COVID-19 in Shenzhen China: Analysis of 391 cases and 1,286 of their close contacts. *medRxiv*, 2020.

- [38] Clément Massonnaud, Jonathan Roux, and Pascal Crépey. COVID-19: Forecasting short term hospital needs in France. *medRxiv*, 2020.
- [39] Santé Publique France. Données hospitalières relatives à l'épidémie de COVID-19, 2020.

A ~~Method~~

The incidence and prevalence data for France were taken from [39]. For a fixed set of parameters, the solution $n(t, a)$ to the McKendrick-von Foerster equation was solved numerically using a Euler scheme and spatial boundary condition making use of $\tau = R_0 \hat{\tau}$ specified by (unknown, to be estimated) R_0 and $\hat{\tau}$ fixed as in (18). The predicted number of deaths, discharges, and ICU/hospital occupied beds were then computed numerically using

$$\forall t \geq 0, \quad n_i(t) = \int_0^\infty n(t, a) p(a, i) da,$$

where $n_i(t)$ is the size of the subpopulation in state i at time t and $p(a, i) = \mathbb{P}(X(a) = i)$, where X is the life process of a typical individual. The predicted incidence in state i between time t and s , denoted by $\tilde{n}_i(t, s)$, can be obtained using the expression

$$\tilde{n}_i(t, s) = n_i(s) - n_i(t) + \sum_j n_j(s) - n_j(t),$$

where the sums is taken over all states j such that the process $(X(a))_{a \geq 0}$ can reach state j after having visited state i . The predicted number of ICU/hospital admissions was computed using this expression.

We considered a Poisson likelihood. More precisely, given the predicted values displayed previously, we assumed that the observed values follow a Poisson distribution whose mean is the corresponding predicted values. We supposed that Poisson observations were independent among days, and among time series. This yields a product-form expression for the likelihood of the data. We then looked for the parameter set that maximizes this likelihood.

The maximum likelihood parameter set was obtained using the `minimize` function of the Python `scipy.optimize` module, using a Nelder-Mead algorithm. We selected as initial point of the optimization algorithm a set of parameters that were close to the existing estimates in the literature, or which seemed realistic if such estimates did not exist.

B ~~Results~~

Recall the admission model from Section 4.4. By adding two parameters to the model, one for the mean time between hospital admission and discharge, the other for the mean time between ICU admission and discharge, we can derive an expression for the likelihood of the prevalence and incidence time series under the admission model. The best-fitting values for these two parameters were obtained by maximizing the likelihood with all other parameters values fixed to those estimated in Table 2. The corresponding model is displayed in Figure 8.

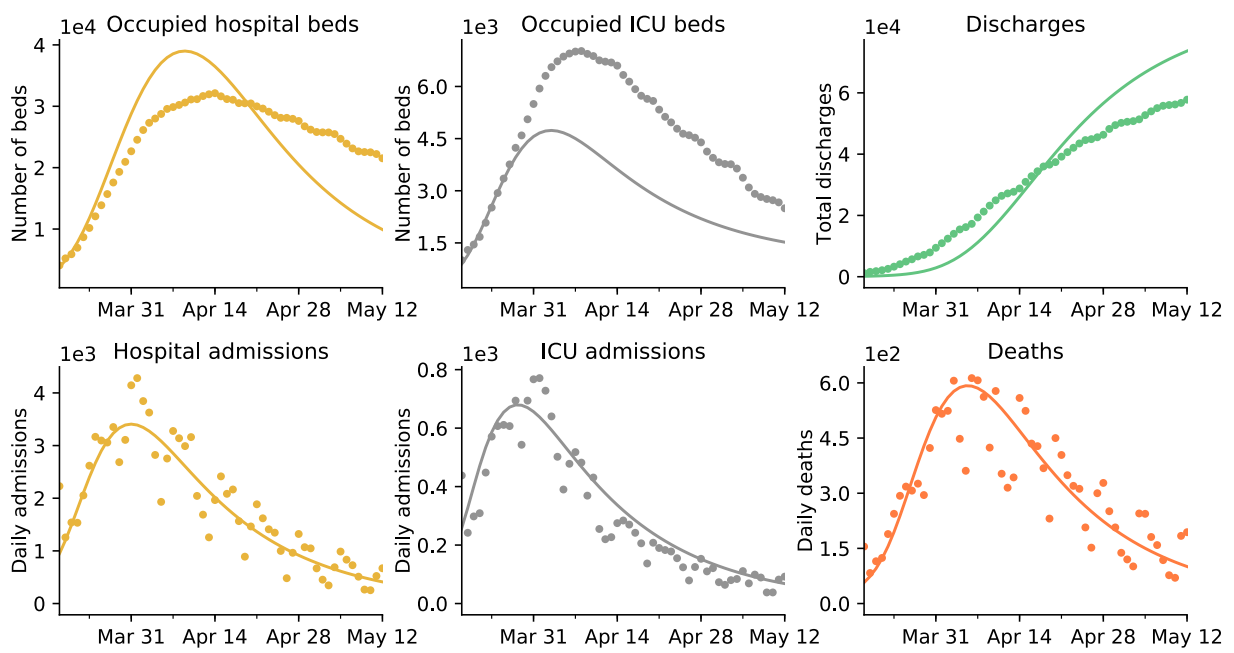


Figure 8: Best fit of the admission model for prevalence data.